LOCALIZATION OF AUTONOMOUS VEHICLES USING RFID PHASE SHIFT

A Thesis

by

BLAKE AUSTIN LEIKER

Submitted to the Office of Graduate and Professional Studies of
Texas A&M University
in partial fulfillment of the requirements for the degree of

MASTER OF SCIENCE

Chair of Committee,	Swaminathan Gopalswamy
Committee Members,	Sivakumar Rathinam
	Behbood Zoghi
Head of Department,	Andreas Polycarpou

May 2019

Major Subject: Mechanical Engineering

ABSTRACT

RFID systems are a commonly used method of identifying objects, and the use of RFID for high precision localization is of growing interest. RFID is a promising method for the unique identification of autonomous vehicles within a larger system, such as infrastructure enabled autonomy. This paper describes a scheme for tracking the location of autonomous vehicles using on-board battery-assisted passive RFID tags. The localization method described relies on the physical principle that the phase of a radio signal varies linearly with the distance between the transmitting and receiving antenna. The measured phase difference is used in conjunction with frequency hopping to overcome the natural ambiguity of the phase measurements to calculate the distance between a single RFID antenna and tag. A Kalman filter was also developed and implemented to demonstrate the performance of the localization method when filtered.

The proposed algorithm was implemented and tested using ROS. The Impinj Speedway R220 RFID reader was used for testing, and communication with the RFID reader was implemented using the Impinj Octane SDK. Testing included both static and mobile experiments. Static tests showed consistent localization out to 40 meters. The Kalman filter successfully removed bad estimates and converged quickly to the true distance. The static tests also confirmed that the algorithm is successful even when the antenna is off-angle from the RFID tag. The mobile experiments did not demonstrate successful localization, likely due to an error when testing which caused only a coarse velocity measurement to be obtained. This experiment will be repeated with a more accurate velocity measurement to determine the effect that movement has upon the described algorithm.

The main contribution of this research is the completely novel, phase-based localization method for RFID. Preliminary experimentation was performed as a proof-of-concept for this approach, but there are still many open-ended questions. Localization was performed between a single tag and a single antenna, but the method could be extended to multi-tag or multi-antenna localization. Additionally, the method still needs to be demonstrated for localization of a mobile tag.

ACKNOWLEDGMENTS

I would like to thank my thesis advisor, Dr. Swaminathan Gopalswamy, who supported this project from start to finish. Additional thanks to Dr. Behbood Zoghi, who provided valuable technical experience in the area of RFID.

CONTRIBUTORS AND FUNDING SOURCES

Contributors

This work was supported by a thesis committee consisting of Professor Swaminathan Gopalswamy and Professor Sivakumar Rathinam of the Department of Mechanical Engineering and Professor Behbood Zoghi of the Department of Engineering Technology and Industrial Distribution.

The data collected for section 3.2 was collected with the help of Tyler Marr of the Department of Mechanical Engineering. All other work conducted for the thesis was completed by the student independently.

Funding Sources

Graduate study was supported by a fellowship from Texas A&M University. This research project was partially funded by the Denso Corporation.

NOMENCLATURE

BAP	Battery-Assisted Passive
COTS	Commercial Off-The-Shelf
EPC	Electronic Product Code
IC	Integrated Circuit
LLRP	Low-Level Reader Protocol
MSSP	Multi-Sensor-Smart-Pack
RFID	Radio Frequency Identification
ROS	Robot Operating System
TAMU	Texas A&M University

TABLE OF CONTENTS

Page

LIST OF FIGURES

FIGURE Page

LIST OF TABLES

TABLE Page

1. INTRODUCTION

Infrastructure enabled autonomy is a proposed paradigm which re-balances the responsibility that current automotive manufacturers hold with potential infrastructure and third-party players [1, 2]. In this proposed system, the infrastructure provides the capability for self and contextual awareness of autonomous vehicles through the use of devices called Multi-Sensor-Smart-Packs (MSSPs). These sensor packs contain various sensors, such as cameras or LIDAR, which allow for autonomous vehicle situational awareness. The accurate identification and localization of vehicles is a crucial and fundamental need for the success of the system, and RFID technology presents a possible solution.

Radio Frequency Identification (RFID) systems are commonly used in logistical and asset-tracking applications due to their low cost compared to other automatic identification technologies. An RFID system in its simplest form consists of RFID tags and RFID readers. The RFID reader uses an antenna to send radio waves to the tag, which responds with an identifier unique to the RFID tag. This technology is widespread across many industries due to the small size and low cost of tags. Location tracking of RFID tags is an open and lively area of research, as the ability to incorporate spatial information into existing RFID systems allows these systems to become faster, more robust, and more efficient. Within the scope of autonomous vehicles, any system tracking and controlling a fleet of vehicles will need a reliable method of identifying vehicles within the system, and RFID provides an obvious and well established solution to this problem. Furthermore, additional localization capabilities will increase the effectiveness of the overall system.

This paper introduces a novel method of RFID based localization which is based solely upon the phase of the tag signal. Because modern off-the-shelf RFID systems are able to report the signal phase, this technique provides a low cost and easily implementable way to localize an object. The method described herein requires only a single antenna and tag to localize an object in theory, but a network of antennas may be used to greatly increase the area of localization. With other comparable systems, an array of antennas or tags is required before any localization is possible.

Additionally, the described system works using active RFID technology. The much longer range offered by active RFID (hundreds of meters in some cases) makes the system viable for use in an autonomous vehicle tracking scenario. The provides system would provide added value to an IEA network because of its ability to uniquely identify multiple vehicles while providing additional localization information.

1.1 Literature Review

Various methods of RFID tag based localization have been attempted. More traditional methods of radio frequency tracking, such as angle of arrival or time of arrival (used by GPS), are generally infeasible because the signal delay of RFID communication is on the order of nanoseconds. The three main pieces of information which are used for RFID-based localization schemes are tag proximity, received signal strength (RSS), and phase. RSS and phase-based methods are viable because RFID readers recover the signal strength and baseband phase, and many modern readers make this information available to the user. Some applications localize a tag, while other applications localize the reader.

Proximity based methods are generally the most simple to implement because they involve only detecting whether an RFID tag is within range of an RFID reader. This method is the most commonly used method in vehicular applications. Perez et al. used a form of RFID proximity localization for an intelligent cruise control system [3]. An RFID reader within the car detected when the vehicle drove passed certain traffic lights, and through networking with the traffic control system the vehicle is able to avoid red lights. Lee et al. also used RFID proximity for localization by using tags placed at known locations to correct GPS signals [4]. Another notable example of proximity-based localization was demonstrated by Roehrig et al., who used an array of RFID tags placed in the floor to localize an autonomous robot equipped with an RFID reader [5].

RSS-based localization is one of the most common methods of RFID localization. Generally, RSS methods use an array of reference tags placed throughout the environment. Comparing the measured RSS to the RSS of reference tags in known locations has been done many times with varying degrees of success [6, 7, 8, 9, 10, 11]. The accuracy of these methods are upwards of one

meter, and they are very environment dependent. These methods also require an initial calibration to be effective in a given environment, and changing hardware can greatly affect RSS readings. The requirement for either reference tags or extensive calibration also makes RSS based methods difficult when localization is necessary over very large areas.

While RSS-based methods have been used successfully, phase-based methods show more potential for highly accurate localization. Nikitin et al. proposed various methods which use the phase of the RFID signal for localization [12]. Some limited success was shown using these methods to localize a single tag. Hekimian et al. also demonstrated very accurate localization using similar methods [13]. DiGiampaolo et al. and Ma et al. both combined the phase-based estimation with RSS fingerprinting methods to achieve very accurate results [14, 15]. The Tagoram system described in [16] also showed great success in using RFID phase to track large quantities of RFID tags. Using commercial off-the-shelf RFID equipment, this system was able to track tags to centimeter level accuracy from up to 10 meters away using only the measured phase. In this paper, we describe a system meant to track mobile RFID tags at long ranges using commercial off-the-shelf RFID technology.

2. METHODOLOGY

2.1 Background Theory

RFID as a technology has become increasingly common in industry in recent years, primarily for the purpose of asset tracking [17]. An RFID system consists of RFID readers, antennas, and tags. The RFID reader is programmable and sends the RF signal through a coxial cable to the antenna, which then transmits the signal, known as the interrogating signal, to the RFID tag. The RFID tag waits until it receives an interrogating signal, which it then re-modulates and sends back to the reader's antenna. The reader decodes the received signal to determine the tag "Electronic Product Code", or EPC, which is a unique number used to identify a specific RFID tag. Other data may also be sent and decoded in addition to the EPC.

Various types of RFID systems exist. They are typically classified into Low Frequency (LF), which operate at 125 kHz, High Frequency (HF), which operate at 13.56 MHz, and Ultra-High Frequency (UHF), which operate at 430 or 860-930 MHz. LF and HF tags are typically very low range and may operate using different physical principles, and this paper focuses only on RFID systems in the UHF range.

Many modern off-the-shelf RFID readers offer advanced features, such as the ability to report measured signal strength and phase. This information greatly increases the ease with which localization systems may be designed and prototyped because the surrounding radio-frequency communication network no longer needs to be developed from scratch.

2.1.1 RFID Tags

RFID tags typically consist of an antenna and an integrated circuit (IC). Ultra-High Frequency tags generally use a simple dipole antenna with a design unique to the tag application. The dipole antenna converts the radio signal sent from the reader into an oscillating electric current, which is then demodulated and interpreted by the IC of the tag. The size of the antennas used can vary greatly, generally depending upon power requirements and the environment in which the RFID

system is to be implemented. The tag integrated circuit contains memory banks which store the tag EPC, user data, and other data which may be used to control various tag functionality.

RFID tags may be either passive, battery-assisted passive, or active. Passive tags are powered using the radio energy of the signal transmitted from the RFID reader. Because they require no internal power source, they can be manufactured very cheaply. Passive tags are very common due to their low cost, but their range is limited by the power of the interrogating signal. Typically, passive tags can have a range of up to several meters in ideal conditions. Active RFID tags are powered by a battery and act as beacons by periodically emitting signals; they do not wait for the interrogating signal from the reader. Because the emitted signal is powered by a battery, active RFID tags have greatly increased range over passive tags (up to 200 meters). Battery-assisted passive (BAP) tags combine the characteristics of passive tags and active tags. BAP tags use a battery to increase the power of the transmitted signal, but the tag only emits a signal in response to an interrogating signal sent by a reader. This increases the battery life of the tag and causes the tag to behave in a predicable way, which may be taken advantage of for localization purposes.

2.1.2 Communication Protocols and Standards

The air interface for UHF RFID tags is defined by the ISO/IEC 18000 standard. This standard specifies information such as the occupied channel bandwidth, modulation, operating channels, frequency hop rate, and hop sequence. Frequency hopping is a method of transmitting radio signals among many different frequency channels. The purpose of frequency hopping is to decrease the effect of interference, both from environmental noise and other devices occupying the same frequency band. Many frequency bands are required by law to employ frequency hopping, and this is true of the 902 - 928 MHz frequency band. FCC regulation 15.247 defines operation in the 902 - 928 MHz band [18]. The regulation specifies that frequency hopping must be used with at least 50 channels, and transmission on a single channel must not last longer than 0.4 seconds. This pseudo-random frequency hopping behavior is an important factor to consider when designing a localization algorithm based upon radio wave propagation characteristics; as will be seen, frequency hopping may actually be leveraged to glean more information from the measured signal

characteristics.

In addition to the air interface protocol, LLRP (Low-Level Reader Protocol) is also used to communicate between the PC and the RFID reader. LLRP defines specific commands that are used to control the operation of an RFID reader. Most RFID readers support LLRP, so existing LLRP packages may be used and extended to develop an application that controls a specific reader. This increases the speed at which applications may be developed, and increases their portability.

2.1.3 Radio-Frequency Physics

Ultra-high frequency RFID tags operate using a method known as backscatter radiation coupling, meaning the reader and the tag communicate through the use of backscatter radiation. Electromagnetic waves are sent through the environment from the reader antenna to the tag antenna, and vice versa. The radiation pattern emitted by the reader antenna can vary depending upon the type of antenna, and this is an early design choice that must be considered when constructing an RFID system.

The properties of the electromagnetic wave propagation may be used to provide information about the location of the tag. RSSI, or received signal strength indicator, is a typical measure of the power of a radio signal. One common model for radio signal power is the Friis transmission equation [19]. This equation relates the measured signal power to the distance between the transmitting and receiving antennas, but there are several reasons why an analytically-derived localization scheme would be difficult using this model. Because the Friis equation assumes that the antennas are correctly aligned and share the same polarization, as well as the assumption that the transmission occurs in free space, it is very difficult to achieve accurate results in an RFID system using purely this model. The free space assumption means that having the antennas close to the ground or near buildings would cause large inaccuracies. In addition, the Friis equation requires knowledge of the power fed into the input terminals of the transmitting antennas, which would be difficult to quantify accurately in the case of an RFID tag because generally the transmission power is dependent upon the strength of the interrogating signal. Accurate localization using this model is most likely not possible because of the effects of the environment upon the measured

signal power. While the Friis equation is purely analytical, other empirical relationships have been established as well which relate the distance between two antennas to the signal strength. Methods such as machine learning may also be used to correlate the tag position to the signal strength, but these methods are still very environment-dependent.

Another useful measure of the radio signal propagation is the phase. While the signal power may be heavily affected by environmental factors, the phase of the signal may be measured very accurately and changes in a much more predictable way. The phase of the received tag signal may be written in the form:

$$\phi = \phi_{prop} + \phi_o, \tag{2.1}$$

where ϕ_{prop} is the phase accumulated due to electromagnetic wave propagation and ϕ_o is the phase offset, which includes phase accumulated from any other sources. The phase offset depends on many different factors, including the modulation properties of the tag and the properties of the various system components, such the antenna cable and other reader components. However, it may be assumed that the phase accumulated from these factors does not change from measurement to measurement, so it is possible for this phase offset to be calibrated out. The phase due to signal propagation through the environment (assuming no environmental effects) is known to be the following:

$$\phi_{prop} = -\frac{4\pi D}{\lambda} \bmod 2\pi, \tag{2.2}$$

Where D is the distance between the reader's antenna and the tag, and λ is the wavelength of the carrier signal. This equation shows that ϕ_{prop} has a simple linear relationship with D. Because of the periodic nature of the phase measurement, the same phase measurement corresponds to many different distances, with the phase repeating every $\lambda/2$ of distance moved. Additionally, off-the-shelf hardware also introduces a phase ambiguity of π, which decreases the discernible distance to $\lambda/4$. For a radio operating at 910 MHz, the distance $\lambda/4$ is equal to approximately 8.2 centimeters. This phase ambiguity is the major difficulty to overcome when formulating phase-based distance measurement techniques. The problem is complicated further if the tag moves farther than $\lambda/4$

between two consecutive phase measurements. The following algorithm attempts to overcome these complications to glean information about the distance between the tag and the antenna.

2.2 Phase Difference Algorithm

In order to approximate the true distance between the tag and the reader antenna, equation 2.2 is reformulated into the following form.

$$\phi_i + 2\pi n_i = -\frac{4\pi D_i}{\lambda_i} + \phi_{o,i} \tag{2.3}$$

The subscript i refers to a particular phase measurement in a series of measurements, where D_i and λ_i are the corresponding distance and wavelength at the time of that particular phase measurement. Note that the wavelength λ_i will be fluctuating over time. The term n_i refers to the "cycle" of the phase measurement and is the integer quotient of the modulo operation. If it is possible to guess the value of n, then the distance may easily be determined. To obtain a guess for n, we take an earlier phase measurement ϕ_j, where $\lambda_j \neq \lambda_i$.

$$\phi_j + 2\pi n_j = -\frac{4\pi D_j}{\lambda_j} + \phi_{o,j} \tag{2.4}$$

Note that the phase offset, ϕ_o, is assumed to be constant for the series of measurements corresponding to λ_i, but the phase offset is not necessarily the same for λ_j. In other words, the phase offset is constant for a single frequency, but as the frequency hops, the phase offset will also change.

Subtracting equation (2.4) from equation (2.3) results in the following:

$$\phi_i - \phi_j + 2\pi n_{ij} = -\frac{4\pi D_i}{\lambda_i} + \frac{4\pi D_j}{\lambda_j} + \phi_{o,ij}, \tag{2.5}$$

Where $n_{ij} = n_i - n_j$ and $\phi_{o,ij} = \phi_{o,i} - \phi_{o,j}$. In order to determine more information about the tag distance, it is assumed that the radial velocity of the tag is readily available. When using this system within the broader scheme of Infrastructure Enabled Autonomy, it is a reasonable assumption that the infrastructure will have access to accurate vehicle velocity information. There are many ways

for the velocity information to be made available to the RFID system, one of which being that the velocity value is injected directly into the RFID signal sent from the tag. Using the given velocity information, it is possible to rewrite the distance D_j in terms of D_i:

$$D_j = D_i - \sum_{m=j}^{i-1} v_m \delta t \tag{2.6}$$

In addition, it is assumed that that phase offset difference $\phi_{o,ij}$ may be calculated at the time of each measurement. This relationship was experimentally determined to be a linear function of frequency, as will be shown in section 3.1.1. Because the frequencies of the measurements are known, $\phi_{o,ij}$ is easy to calculate in real time. This relationship is shown below.

$$\phi_{o,ij} = \phi_{o,i} - \phi_{o,j} = m * (f_i - f_j), \tag{2.7}$$

Where m is the slope of the relationship and has been experimentally determined.

Using the relationship of equation 2.6, equation (2.5) may be rewritten into the following form:

$$\phi_i - \phi_j + 2\pi n_{ij} = -4\pi D_i \left(\frac{1}{\lambda_i} - \frac{1}{\lambda_j} \right) - \frac{4\pi}{\lambda_j} \sum_{m=j}^{i-1} v_m \delta t + \phi_{o,ij} \tag{2.8}$$

The true value of D_i is unknown because the true value of n_{ij} is unknown; however, using multiple measurements, the true value of n may be guessed. To do this, D_i may be calculated for various candidate values of n_{ij}:

$$D_i = \left(\phi_i - \phi_j + 2\pi n_{ij} + \frac{4\pi}{\lambda_j} \sum_{m=j}^{i-1} v_m \delta t - \phi_{o,ij} \right) / \left(4\pi \left(\frac{1}{\lambda_i} - \frac{1}{\lambda_j} \right) \right) \tag{2.9}$$

Because it is known that every value of n must be an integer, each calculated D_i may be used to calculate n for another time step k, where $\lambda_k \neq \lambda_j \neq \lambda_i$.

$$n_{ik} = (\phi_k - \phi_i + \phi_{o,ik})/2\pi + 2D_i \left(\frac{1}{\lambda_k} - \frac{1}{\lambda_i} \right) - \frac{2}{\lambda_k} \sum_{m=k}^{i-1} v_m \delta t \tag{2.10}$$

If this calculated value of n_{ik} is an integer, then it is likely that the value of D_i used is the true value. Thus, the algorithm is as follows:

1.	Guess a value of n_{ij}.
2.	Calculate D_i using equation (2.9).
3.	Calculate n_{ik} using equation (2.10).
4.	Repeat 1,2,3 for various integer values of n_{ij}.
5.	Return D_i that corresponds to the n_{ik} that is closest to an integer value.

Table 2.1: Localization Algorithm.

This is performed for every measurement of phase ϕ_i that is received. Assuming no measurement noise and that the transmission occurs in free space, this will perfectly return the distance between the two antennas at each phase measurement. Typically, there is one value of D_i which is very close to the true value, and the trick is getting the algorithm to return that value.

For better performance with noisy measurements, the algorithm is repeated at each measurement ϕ_i for multiple values of ϕ_j and ϕ_k and the results are averaged. This requires that multiple phase values are obtained at each frequency, which is generally possible. This greatly increases the accuracy of the distance estimation.

In addition to using repeated measurements, a cost function was implemented to further reject outliers and choose guesses which are more likely to be accurate. In addition to using the distance to the nearest integer for n_{ik}, the cost function also prioritizes values which are closer to a moving average of the previous values, which helps outlier rejection. The calculated value of D_i which has the lowest calculated cost value is chosen at each time step.

$$S = |round(n_{ik}) - n_{ik}| + \beta * |D_i - moving\_average(D)| \tag{2.11}$$

where β is a design constant used to scale the relative effect of each term. The first term is the distance to the nearest integer for n_{ik}, and the second term is the distance of the current candidate

distance value to a moving average of the previously calculated distance values. This extra term helps to reject any candidate values which are a large distance away from the previous values, so that outliers are less likely to be selected. Thus, the updated algorithm is given below.

1.	Guess a value of n_{ij}.
2.	Calculate D_i using equation (2.9).
3.	Calculate n_{ik} using equation (2.10).
4.	Repeat 1,2,3 for various integer values of n_{ij}.
5.	Return D_i that returns the minimum cost function value S.

Table 2.2: Localization Algorithm with Cost Function.

2.3 Kalman Filter

A filter was also developed to demonstrate the performance of the proposed algorithm when filtered. Because this distance estimate is a measurement of a stochastic dynamic system, a Kalman filter is a good choice of estimator [20]. The Kalman filter is a common type of filter used to estimate the state of linear systems. The Kalman filter is in essence a two step recursive filter. The first step of the filter predicts the state of the system using the assumed dynamic behavior, while the second step updates the prediction using measurements of the state.

Because the quantity of interest is the distance between the reader antenna and the RFID tag, the state of the system is taken to be the distance, D, and the change is distance with respect to time, $\dot{D}$. This is shown below in equation 2.12.

$$x = \begin{bmatrix} D \\ \dot{D} \end{bmatrix} \tag{2.12}$$

This Kalman filter will assume a simple linear system where a change in velocity is caused by an

unknown process noise. The state update equation is shown below in equation 2.13.

$$x_{k+1} = \begin{bmatrix} 1 & \Delta t \\ 0 & 1 \end{bmatrix} x_k + \begin{bmatrix} 0 \\ 1 \end{bmatrix} w_k \tag{2.13}$$

The process noise is assumed to be a normally distributed, stochastic random variable of mean 0 and variance σ_w^2. This is expressed by equation 2.14.

$$w_k \sim N(0, \sigma_w^2) \tag{2.14}$$

Because the algorithm itself requires a measurement of the velocity, the entire state is available to be measured. The system measurement is corrupted by some measurement noise, v_k, which is assumed to be a stochastic random variable. The measurement equation of the system is given by equation 2.15.

$$z_k = \begin{bmatrix} 1 & 0 \\ 0 & 1 \end{bmatrix} x_k + v_k \tag{2.15}$$

The covariance of v_k is assumed to be to be diagonal for the purposes of this filter, although in reality the errors of each measurement are not unrelated. This is shown in the equation below.

$$v_k \sim N(0, \begin{bmatrix} \sigma_{z1}^2 & 0 \\ 0 & \sigma_{z2}^2 \end{bmatrix}) \tag{2.16}$$

This formulation of the Kalman filter contains two steps. The *a priori* step, shown in equation 2.17, updates the state estimate $\hat{x}$ and the state error covariance P using the system dynamics. The *a posteriori* step, shown in equation 2.18, updates the state estimate and error covariance to take into account the most recent measurement. These calculations are performed each time a new

measurement is made to obtain the expected value of the state.

$$\begin{aligned} P_{k+1}^{-} &= AP_kA^T + GQG^T \\ \hat{x}_{k+1}^{-} &= Ax_k \end{aligned} \tag{2.17}$$

$$\begin{aligned} P_{k+1} &= [(P_{k+1}^{-})^{-1} + H^T R^{-1} H]^{-1} \\ \hat{x}_{k+1} &= \hat{x}_{k+1}^{-} + P_{k+1} H^T R^{-1} (z_{k+1} - H\hat{x}_{k+1}^{-}) \end{aligned} \tag{2.18}$$

This estimate of the distance D tends to be more accurate than the raw estimation provided by the algorithm. Different formulations could also be implemented which include more accurate vehicle dynamics. This filter was developed mainly to present an example of filtered data as a demonstration of the capabilities of the proposed localization algorithm.

2.4 Implementation

2.4.1 Experimental Apparatus

In order to perform an experimental validation of the proposed algorithm, equipment was purchased to develop a proof of concept system. An Impinj Speedway R220 RFID reader was chosen to be used for all testing, shown below in figure 2.1. One reason that this RFID reader was chosen was because of its robust software development kit, Octane SDK. Octane SDK is a C# framework and it allowed for software to be developed and implemented much quicker than implementing LLRP directly. Octane SDK is an Impinj implementation of LLRP that has been extended to include extra features of the Speedway reader. One of these extra features that was useful for this project is RF phase and RSSI reporting capabilities. The phase is required to be measured using this tag localization scheme, and the Impinj Speedway made this information easily available with every tag read.

Figure 2.1: Impinj R220 RFID Reader.

This reader uses an operating frequency range of 902-928 MHz, which is common for UHF RFID. As previously mentioned, any device operating in this frequency range is required to hop between at least 50 channels at a rate of at least 1 channel every 0.4 seconds. It was found through initial testing that the Speedway operates over 50 channels evenly spaced at 0.5 MHz, and that it hops between channels every 0.2 seconds.

The Speedway has a listed read rate of 200 tags per second, although the highest encountered read rate was much lower than this during testing. This reader also uses a monostatic antenna configuration, which means that the transmitting antenna and the receiving antenna are the same. This is as opposed to a bistatic or multistatic antenna configuration, in which different antennas are used for transmitting and receiving. Generally, RFID systems are monostatic, and the proposed algorithm assumes this to be true.

The chosen antenna was the MTI MT-262006 outdoor antenna, shown below in figure 2.2. This antenna is circularly polarized with a 63 by 63 degree beamwidth and also operates in the 902-928 MHz frequency range. This antenna is meant for outdoor use and comes with a mounting bracket that allows for mounting the antenna in any orientation. This antenna was chosen because it is widely used in outdoor RFID systems and because it easily pairs with the Impinj Speedway reader using an RP-TNC antenna cable.

Figure 2.2: MTI MT-262006 Outdoor Antenna.

The Confidex Survivor B RFID tag was used for testing because it was the most readily available battery-assisted passive tag on the market. The listed maximum range for this tag is up to 60 meters, although the read rate does decrease at larger distances. The Survivor B is meant to be a rugged, outdoor tag which can be used in difficult environments. Additionally, this tag is applicable to metal surfaces.

Figure 2.3: Confidex Survivor B Battery-Assisted Passive RFID Tag.

The Survivor B uses the EM4325 integrated circuit, which offers programmable user memory. The chip comes pre-programmed with a 96-bit EPC. This chip also supports SPI communication. In theory, a vehicle could be connected to a tag such as this and write velocity information to the chip memory in real time, which would then be transmitted to the reader. Although this idea was investigated for feasibility, no implementation was attempted.

2.4.2 Software

The Octane SDK framework was used in C# to facilitate communication between the main computer and the RFID reader. This was implemented in the software package *rfid_comm*. *rfid_comm* starts the reader and adjusts the settings so that tags are read as fast as possible. The reader reports back to the application each time a tag is read, and various information is contained within this read report. The only information used in this testing application was the read time, transmission frequency, antenna number, tag EPC, and the measured phase. The *rfid_comm* application also acts as a data server. All data that the application receives from the RFID reader is broadcast over TCP to any client connections. This was done in order to separate the reader communication process from the tag localization; all localization calculations are performed outside of *rfid_comm*. The *rfid_comm* application also has the capability to read and write to an RFID tag's memory, but this capability is not in use during most experimentation.

The RFID localization was implemented using the Robot Operating System (ROS). A single ROS package was created named *rfid_localization*. This package consists of one main node, *tag_tracker*, which connects to *rfid_comm* over TCP and performs the localization algorithm. Another node was also developed, *kf_node*, which is an implementation of the Kalman filter described in section 2.3. This is a simplistic filter that makes very little assumptions about the dynamics of the system; its main purpose is to demonstrate the capabilities of this localization technique when used with a filter. In a system such as IEA, a more complex filter could be used to fuse this estimate with other measurements.

The overall software architecture is shown below in figure 2.4. The RFID reader communicates with the RFID using the EPC Gen 2 air protocol. Data from each tag communication is then sent over LLRP to the *rfid_comm* application. The *rfid_comm* application then sends this raw data over TCP to the ROS node *tag_tracker*. The node *tag_tracker* uses the measured phase and frequency data (collected initially by the reader) to perform the tag localization algorithm. This distance estimate is subscribed to by the node *kf_node*, which filters the data using the distance and velocity estimates.

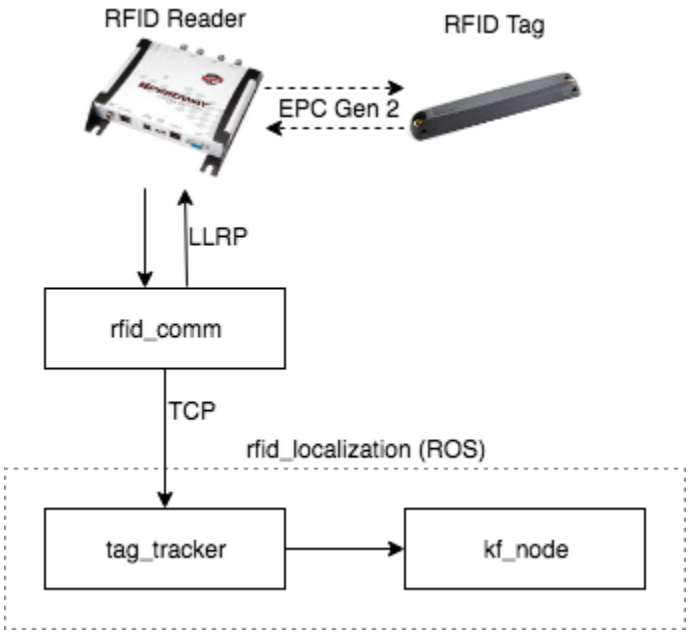

Figure 2.4: RFID System Software Diagram.

3. RESULTS

All testing was performed with a single RFID reader, antenna, and tag using the equipment discussed in section 2.4.1. Performance of the algorithm was initially confirmed using measurements of a completely static tag. A second set of testing was then performed with the tag attached to a vehicle, with data taken at various speeds. All testing was done at the Texas A&M System Rellis campus on an open runway, so that there were no nearby buildings or other obstructions. Although testing was done in an open area, both the antenna and the tag were located only three to four feet off the ground, which may have had some affect on the signal propagation. Although the Confidex RFID tags have a listed range of up to 60 meters, consistent reads were only obtained out to roughly 50 meters. It was found during initial development that the length of the antenna cable has a large effect on the distance at which tags may be read; roughly speaking, a 25 foot cable could read tags at approximately half the distance of a 5 foot cable. All testing was performed using a 5 foot antenna cable, although a longer range likely could have been obtained using either or shorter cable or a higher gain antenna.

3.1 Static Testing

Static testing was performed in which an RFID tag was placed at known distances from the reader and measurements were taken without any tag movement. At each distance, measurements were taken for roughly 20 seconds. Data was taken with the tag at distances of 2, 4, 6, 8, 10, 15, 20, 25, 30, 35, and 40 meters. Plots from all trials of static testing are given in Appendix A.

Figure 3.1 below shows the calculated distance versus time for a single tag at a distance of 30 meters. Both the "raw" calculated distance as well as the filtered distance are shown, where the raw distance is the distance returned from the algorithm and the filtered distance is the distance returned by passing this data through the Kalman filter discussed in section 2.3. Each point corresponds to a new tag read returned from the RFID reader. Tag reads occurred at roughly 30 Hz, although small gaps may be seen in the plot where tag reads slowed down.

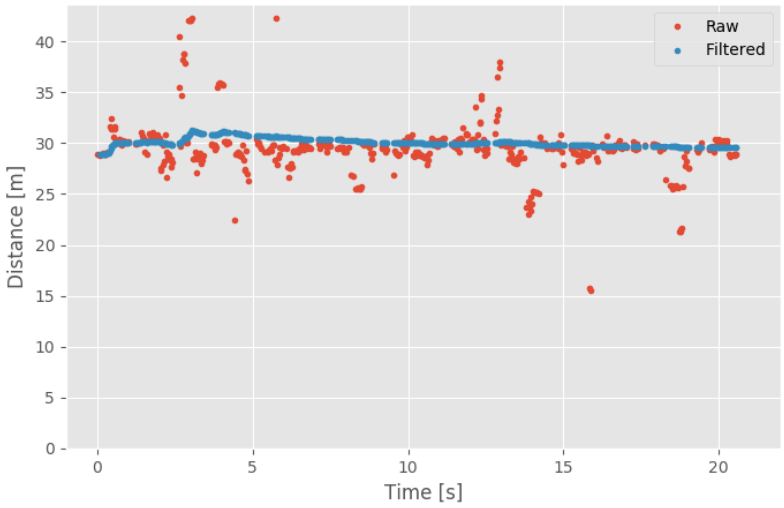

Figure 3.1: Calculated Distance vs. Time for D = 30 m.

This data shows that the tag has been localized accurately to a distance of 30 meters using the proposed algorithm. The Kalman filter converged quickly and successfully attenuated the worst of the estimated points. The steady state error of the filtered signal is less than one meter.

Data taken at 25 meters is shown below in figure 3.2. This data is noisier than the data shown above, and there is a very large error in the initial distance estimate. This large initial error is likely because the the cost function in the algorithm "rewards" guesses which are closer to previous values, and early values do not have previous data points to compare themselves to. However, even with this initial error, the algorithm converges quickly to the true value. Generally, the outliers in the plot are due to incorrect guesses in the algorithm calculation. The values in the cost function were tuned so that the correct guess is chosen the majority of the time, but measurement noise causes some incorrect guesses.

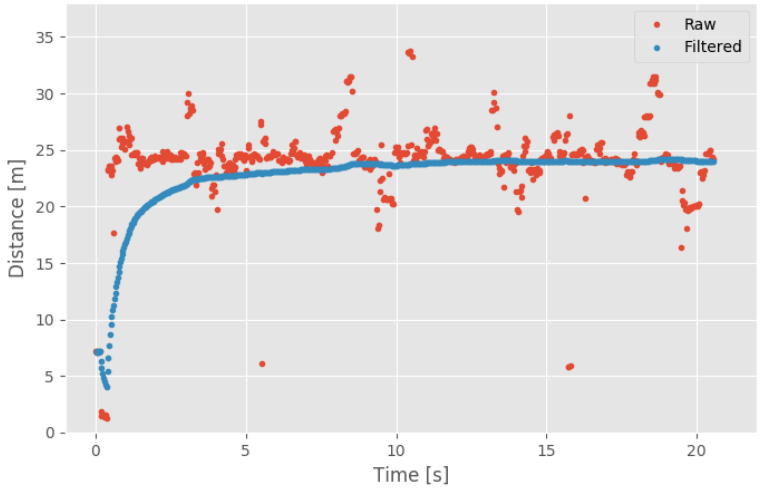

Figure 3.2: Calculated Distance vs. Time for D = 25 m.

Measurements were also taken with the antenna pointing off-angle from the RFID tag to test that the angle at which the antenna is facing the tag does not affect the localization process. These results are shown below in figures 3.3 and 3.4. At 30 meters, changing the angle of the antenna away from the tag noticeably affects the tag read rate. However, even with the lowered read rate, localization is still fairly accurate. Also note that the angle was an approximate measurement; this was done as a way to qualitatively test that localization also functions when the antenna is off-angle from the tag.

Plots for all test data are included in appendix A. In general, the proposed algorithm was successful at localizing the RFID tag while the tag is not moving. Although there were no buildings close by, testing was performed in a fairly realistic environment in which multipath may have been a factor due to the antennas being so close to the ground. Measurements were also taken using another RFID tag to verify that the trends that were seen were not specific to a single tag. The algorithm performed equally as well using the other RFID tag. Additionally, measurements were taken with the antenna angled at 22 and 44 degrees away from the tag. Although the angle of the antenna had a noticeable affect on the range at which tags may be read, it did not appear to affect the localization process.

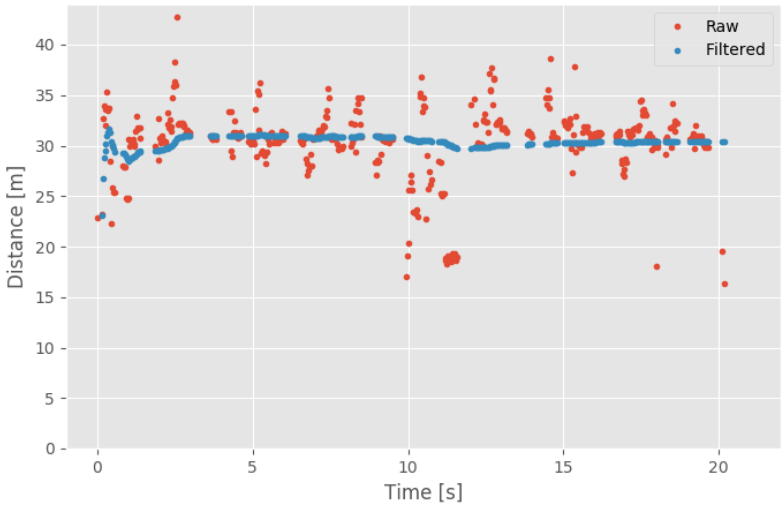

Figure 3.3: Calculated Distance vs. Time for D = 30 m with an antenna angle of 22 degrees.

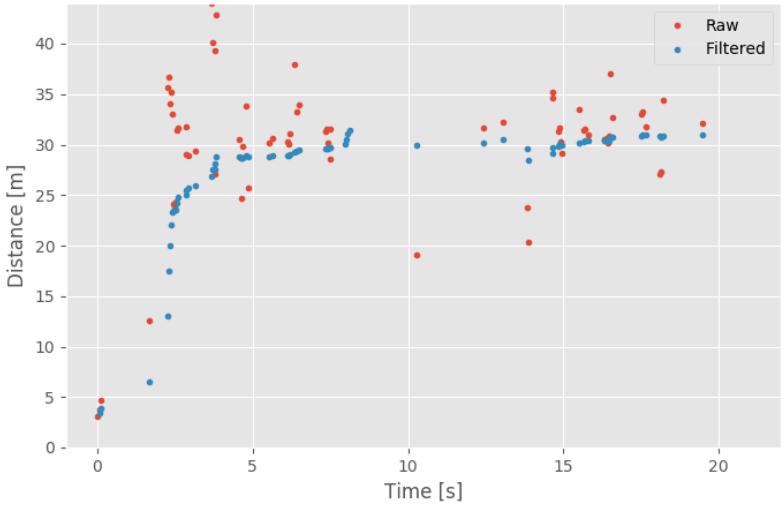

Figure 3.4: Calculated Distance vs. Time for D = 30 m with an antenna angle of 45 degrees.

3.1.1 Phase Offset

As discussed in section 2.2, testing showed that the phase offset of the signal, ϕ_o, is not independent of frequency. The phase offset relationship was characterized using the static test data.

Generally, the phase offset is unknown, but if the distance is known then the phase offset may be calculated. Rearranging equation 2.3 to solve for ϕ_o gives the following equation:

$$\phi_o = \phi + \frac{4\pi D}{\lambda} \mod \pi \tag{3.1}$$

This calculation was performed for each phase measurement taken and plotted versus the transmission frequency to obtain the phase offset relationship. This calculation for the data taken at a distance of 2 meters is shown below in figure 3.5. Generally the measurements are very tightly grouped at each frequency, showing that there is little noise in the signal. At longer distances, a similar trend is shown, but the spread of the points increases greatly.

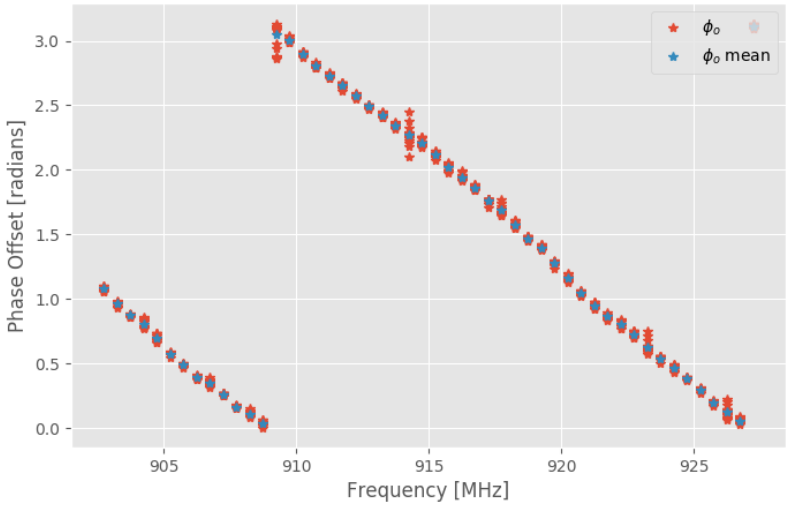

Figure 3.5: Calculated Phase Offset ϕ_o vs. Frequency for D = 2 m.

To determine the exact relationship, a linear regression was performed of the mean of the calculated phase offset at each frequency. This is shown below in figure 3.6.

Therefore, the phase offset has a relationship of the form $\phi_o = m * f + b \mod \pi$. Although the constant b appears to change with time, it is not necessary in the algorithm equations because

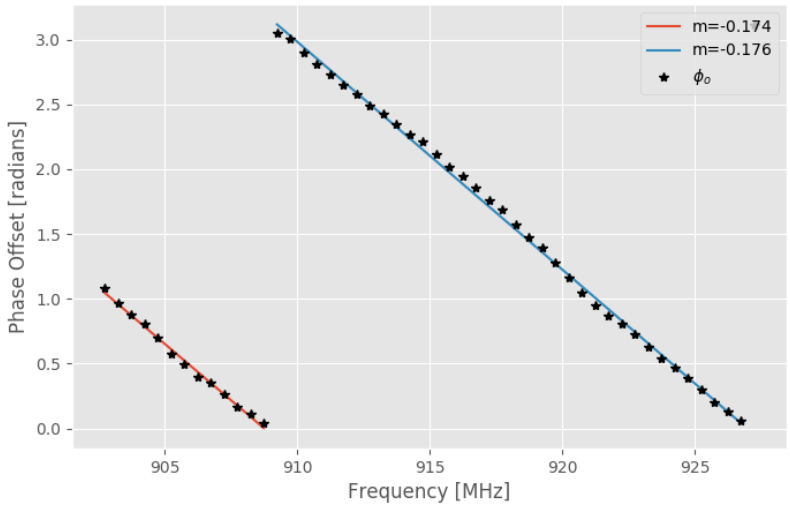

Figure 3.6: Calculated Phase Offset ϕ_o vs. Frequency for D = 2 m with linear regression.

the only value that is necessary to calculate is $\phi_{o,ij}$. The constant b is removed from this equation, and you are left with

$$\phi_{o,ij} = m * (f_i - f_j) \mod \pi \tag{3.2}$$

This empirical relationship was verified using the static test data from multiple other distances, but generally the data became noisier as the distance increased. This $\phi_{o,ij}$ calculation was used to calculate the distance estimate for all test data.

3.2 Dynamic Testing

After the algorithm was developed using the static test data, a second set of testing was performed to determine the performance of the algorithm while the tag is moving. To perform this mobile test, an RFID tag was attached to back of a Lincoln MKZ. The vehicle was equipped with a Swift Piksi differential GPS, which provides centimeter level accuracy. The Piksi provides the distance between a base station and a mobile station, so it is perfectly suited to determine the true distance between the RFID tag and antenna in real time. The Piksi also publishes its position data as a ROS node, which means that it was simple to integrate with the *rfid_localization* package.

Because the mobile station is what publishes the position data, the base station and the mobile station were switched so that the typically "mobile" station could publish its data while remaining next to the RFID reader and antenna. This removed the need for networking and determining timing between multiple computers. This caused a problem in testing, however, because while the mobile station updates its position at 10 Hz, the base station only updates its position at 0.5 Hz. Thus, the true position only appeared to update itself every 2 seconds. The distance algorithm requires the velocity at each time step, and this course measurement of the velocity caused large errors in the distance estimation.

Figure 3.7 below shows the results of the first test performed with the moving tag. Because the velocity of the tag is changing over time, the velocity profile of the tag is shown as well. Note that the time axes match on each plot. Because the velocity is only known at every 2 seconds, but the algorithm requires the velocity at every time step, the velocity was interpolated between the known points at the time of each phase measurement. These interpolated points are shown in blue in the velocity plot. These interpolated velocity points are used in each distance calculation, shown in orange in the upper plot. There appears to be no correlation between the calculation points and the true distance. The data was also filtered using the Kalman filter previously discussed, and this filter did not converge to the true value even when using the accurate velocity measurements.

As can be seen in the figure, the algorithm was unable to correctly predict the tag distance even at very slow speeds. During this test, the vehicle was moving as slowly as possible, but the

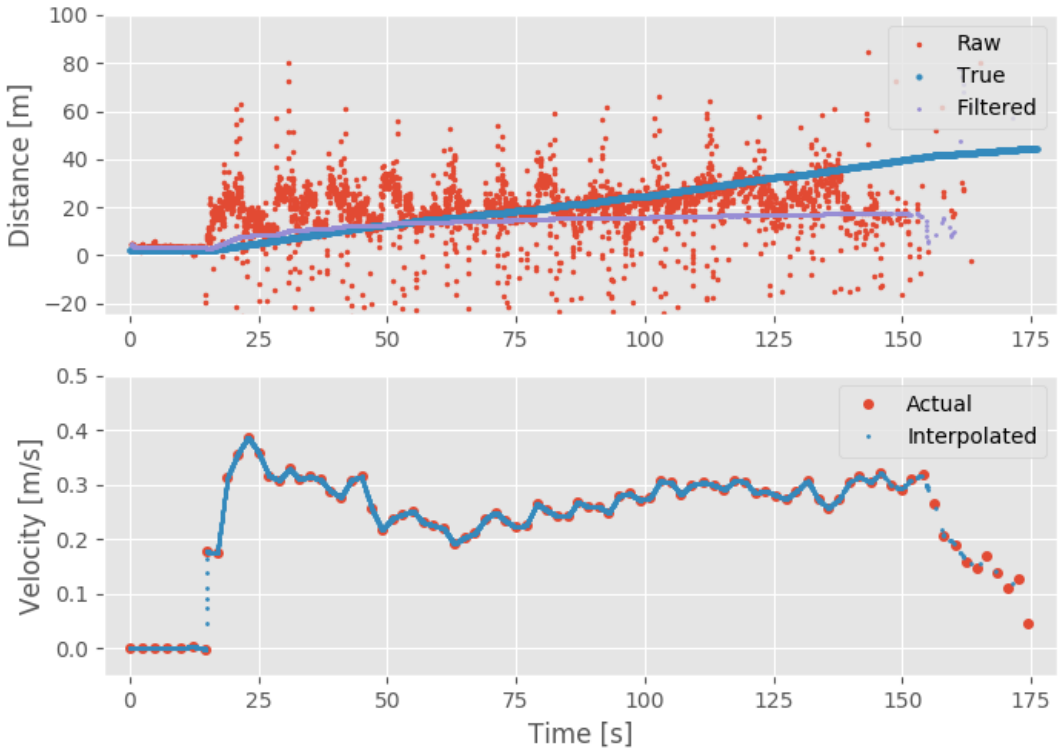

Figure 3.7: Dynamic Test - Trial 1.

estimation was still very poor. Other tests were performed in which the vehicle started from outside of the range of the reader and moved towards the antenna. One such test is shown below in figure 3.8. No reads were obtained until the tag was approximately 40 meters from the antenna. It was repeatedly seen in testing that longer ranges were reached when the tag was first encountered at close distances. This is most likely to the automatic optimization of tag interrogation by the RFID reader; it does not begin aggressively checking for tags until a tag has been encountered.

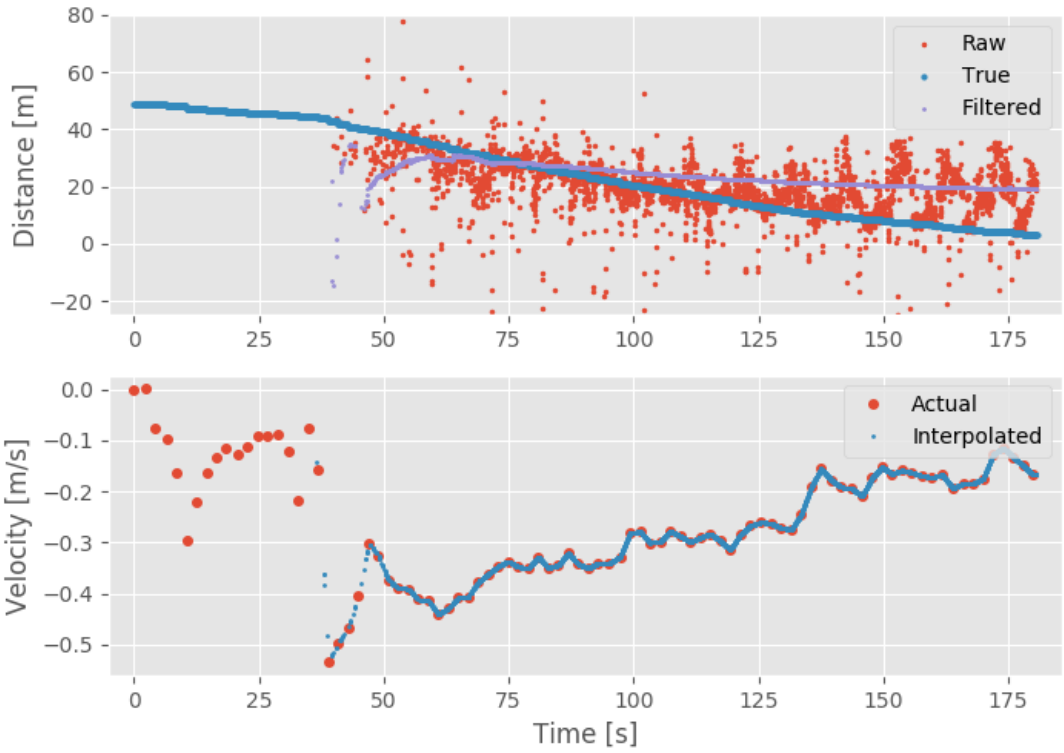

Figure 3.8: Dynamic Test - Trial 3.

It is apparent from the figure that localization was still very poor, with no apparent correlation between the calculated and true distance. More test data is shown in appendix B for various other speeds, with the tag moving both towards and away from the antenna, but successful localization was never achieved. Because of the error in the update rate of the GPS, meaningful conclusions cannot be drawn about this data at this time. Further testing will be performed to determine if a finer velocity measurement allows for localization of a moving tag.

4. CONCLUSIONS

4.1 Summary

RFID technology is widely used to track and identify various objects. This technology has been investigated for use with a system such as IEA, in which the infrastructure provides the capacity for autonomy. RFID technology may be readily used to uniquely identify vehicles, but the effectiveness of the system is greatly increased if localization is also performed. Using RFID for localization has been investigated in various forms, but current methods have many drawbacks which would make implementation infeasible when used in the context of autonomous vehicles. This paper proposes a novel algorithm which uses the phase of the RFID signal to localize an RFID tag. Proof-of-concept experiments were performed which demonstrated successful localization on a single, non-moving RFID tag. Localization of a mobile tag has not yet been demonstrated, but is being pursued. The proposed method shows large promise in the application of vehicle tracking, but long-range RFID tracking could be used in many other contexts. There are also still many open-ended questions regarding this method, and there are many challenges to be overcome.

4.2 Challenges and Future Work

A major problem encountered during testing was the slow update rate of the GPS during the dynamic testing. This error occurred because the base station and the mobile station of the Piksi GPS were switched, so this issue should be easily remedied. Testing showed that even a small error in velocity causes large errors in the phase equation, so it is very important to have the real-time velocity at the time of each phase measurement. Redoing the dynamic testing will determine if the algorithm proposed in this paper is acceptable for use on a mobile tag, or if further adjustments will need to be made. The original goal of the dynamic testing was to determine the top speed at which the tag could successfully be localized, so this question is still open.

Another problem that was encountered was that the length of the antenna cable has a large effect on the strength of the reader signal, and therefore the maximum range at which tags may

be read. The system was tested using a 5 foot and a 25 foot antenna cable, and the 5 foot cable had roughly double the range of the 25 foot cable. While the testing done thus far was done mainly as a proof of concept for the developed algorithm, if this system were to be implemented in an IEA system, the antenna would be located high above the ground on an RSU. The reader would need to be located next to the antenna on top of the RSU, which would be difficult to accomplish with an off-the-shelf RFID system. Implementing this in a practical form would likely require that the RFID system be developed by scratch using a solution such as software-defined radio (SDR). SDR would reduce the total form factor of the system, and it would also allow the different software components to be bundled on one computer rather than having a separate RFID reader which much communicate with a PC. Using SDR would also give much more freedom in many different aspects of the radio communication, such as how frequency hopping is performed. Hopping more frequently than 0.2 seconds could decrease the effect that velocity has upon the phase equation. This would provide many avenues for experimentation and refinement of the proposed localization. Additionally, using SDR could greatly increase the tag read rate, which would increase the effectiveness of the localization algorithm.

The dependency of the algorithm upon the live velocity of the tag is another major challenge. Acquiring the live velocity could be difficult to implement in many potential applications, although in a system such as IEA this information may already be available. The need for an external network to transmit the velocity information could be eliminated by transmitting the live velocity of the vehicle directly in the tag signal. RFID tag integrated circuits such as the EM4325 offer user memory as well as SPI bus support, which could be used to transmit any desired information. The on-board computer of the vehicle could continuously write the velocity of the vehicle to the memory of the tag, which would then be sent every time the reader interrogates the tag. This would present additional difficulties, however, because the radial velocity from the RFID antenna must then be estimated from the tangential velocity of the vehicle. Implementing this method would also require a custom RFID tag design which had an available SPI connection, but this could provide another avenue for improvement. While the Confidex RFID tags used in this paper have a max

range of 60 meters, many active tags have ranges of hundreds of meters. Creating a custom tag would challenging, but could produce better results than any available commercial solution.

Another possible solution to the live velocity problem may be to calculate the velocity of the tag directly from the raw phase measurements, which would completely circumvent the need for a separate velocity measurement. Nikitin et al. discuss a simple method for calculating the radial velocity of an RFID tag using only phase measurements [12]. This calculation would augment the algorithm discussed in this paper, but the feasibility of this solution has not yet been investigated. This method would have the additional benefit that it is the radial velocity that is being calculated, so additional estimation would not need to be performed to convert the vehicle speed.

As exemplified by these many practical challenges, there is still much work to be done to make this system feasible for use in a real-world scenario. Many more scenarios still remain to be investigated, such as testing at different antenna angles, localizing a tag which is moving tangentially to the antenna, or localizing a tag which is near other objects in the environment. The testing discussed in this paper provides a strong basis for further research into this RFID localization scheme.

REFERENCES

[1] S. Gopalswamy and S. Rathinam, "Infrastructure Enabled Autonomy: A Distributed Intelligence Architecture for Autonomous Vehicles," *arXiv:1802.04112 [cs]*, Feb. 2018. arXiv: 1802.04112.

[2] A. Birch, S. Saripelli, and S. Gopalswamy, "Infrastructure Enabled Autonomy for Vehicles," (Maui, Hawaii, USA), Nov. 2018.

[3] J. Perez, F. Seco, V. Milanes, A. Jimenez, J. C. Diaz, and T. d. Pedro, "An RFID-Based Intelligent Vehicle Speed Controller Using Active Traffic Signals," *Sensors (Basel, Switzerland)*, vol. 10, no. 6, p. 5872, 2010.

[4] E.-K. Lee, S. Y. Oh, and M. Gerla, "RFID assisted vehicle positioning in VANETs," *Pervasive and Mobile Computing*, vol. 8, pp. 167–179, Apr. 2012.

[5] C. Roehrig, A. Heller, D. Hess, and F. Kuenemund, "Global Localization and Position Tracking of Automatic Guided Vehicles using passive RFID Technology," in *ISR/Robotik 2014; 41st International Symposium on Robotics*, pp. 1–8, June 2014.

[6] A. K. M. M. Hossain, Y. Jin, W. Soh, and H. N. Van, "SSD: A Robust RF Location Fingerprint Addressing Mobile Devices' Heterogeneity," *IEEE Transactions on Mobile Computing*, vol. 12, pp. 65–77, Jan. 2013.

[7] F. Seco, A. R. Jimenez, and X. Zheng, "RFID-based centralized cooperative localization in indoor environments," in *2016 International Conference on Indoor Positioning and Indoor Navigation (IPIN)*, pp. 1–7, Oct. 2016.

[8] J. Wang and D. Katabi, "Dude, Where's My Card?: RFID Positioning That Works with Multipath and Non-line of Sight," in *Proceedings of the ACM SIGCOMM 2013 Conference on SIGCOMM*, SIGCOMM '13, (New York, NY, USA), pp. 51–62, ACM, 2013. event-place: Hong Kong, China.

[9] X. Huang, R. Janaswamy, and A. Ganz, "Scout: Outdoor Localization Using Active RFID Technology," in *2006 3rd International Conference on Broadband Communications, Networks and Systems*, pp. 1–10, Oct. 2006.

[10] P. Yang, W. Wu, M. Moniri, and C. C. Chibelushi, "Efficient Object Localization Using Sparsely Distributed Passive RFID Tags," *IEEE Transactions on Industrial Electronics*, vol. 60, pp. 5914–5924, Dec. 2013.

[11] Y. Zhao, Y. Liu, and L. M. Ni, "VIRE: Active RFID-based Localization Using Virtual Reference Elimination," in *2007 International Conference on Parallel Processing (ICPP 2007)*, pp. 56–56, Sept. 2007.

[12] P. V. Nikitin, R. Martinez, S. Ramamurthy, H. Leland, G. Spiess, and K. V. S. Rao, "Phase based spatial identification of UHF RFID tags," in *2010 IEEE International Conference on RFID (IEEE RFID 2010)*, pp. 102–109, Apr. 2010.

[13] C. Hekimian-Williams, B. Grant, X. Liu, Z. Zhang, and P. Kumar, "Accurate localization of RFID tags using phase difference," in *2010 IEEE International Conference on RFID (IEEE RFID 2010)*, pp. 89–96, Apr. 2010.

[14] E. DiGiampaolo and F. Martinelli, "Mobile Robot Localization Using the Phase of Passive UHF RFID Signals," *IEEE Transactions on Industrial Electronics*, vol. 61, pp. 365–376, Jan. 2014.

[15] H. Ma and K. Wang, "Fusion of RSS and Phase Shift Using the Kalman Filter for RFID Tracking," *IEEE Sensors Journal*, vol. 17, pp. 3551–3558, June 2017.

[16] L. Yang, Y. Chen, X.-Y. Li, C. Xiao, M. Li, and Y. Liu, "Tagoram: real-time tracking of mobile RFID tags to high precision using COTS devices," in *Proceedings of the 20th annual international conference on Mobile computing and networking - MobiCom '14*, (Maui, Hawaii, USA), pp. 237–248, ACM Press, 2014.

[17] R. Want, "An introduction to RFID technology," *IEEE Pervasive Computing*, vol. 5, pp. 25–33, Jan. 2006.

[18] CFR, "Operation within the bands 902-928 MHz, 2400-2483.5 MHz, and 5725-5850 MHz."

[19] R. C. Johnson and H. Jasik, eds., *Antenna engineering handbook*. New York, NY: McGraw-Hill, 2. ed ed., 1984. OCLC: 10489292.

[20] F. L. Lewis, L. Xie, D. Popa, and F. L. Lewis, *Optimal and robust estimation: with an introduction to stochastic control theory*. No. 26 in Automation and control engineering, Boca Raton: CRC Press, 2nd ed ed., 2008. OCLC: ocm85692880.

APPENDIX A

STATIC TESTING FIGURES

Additional plots for the static testing discussed in section 3.1.

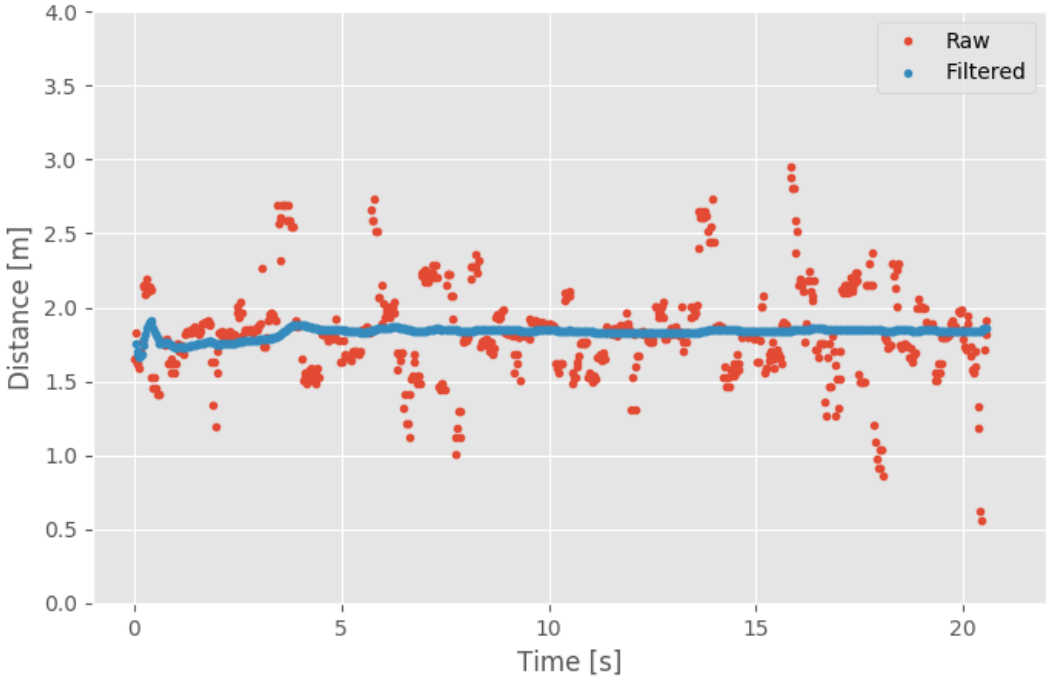

Figure A.1: Calculated Distance vs. Time for D = 2 m.

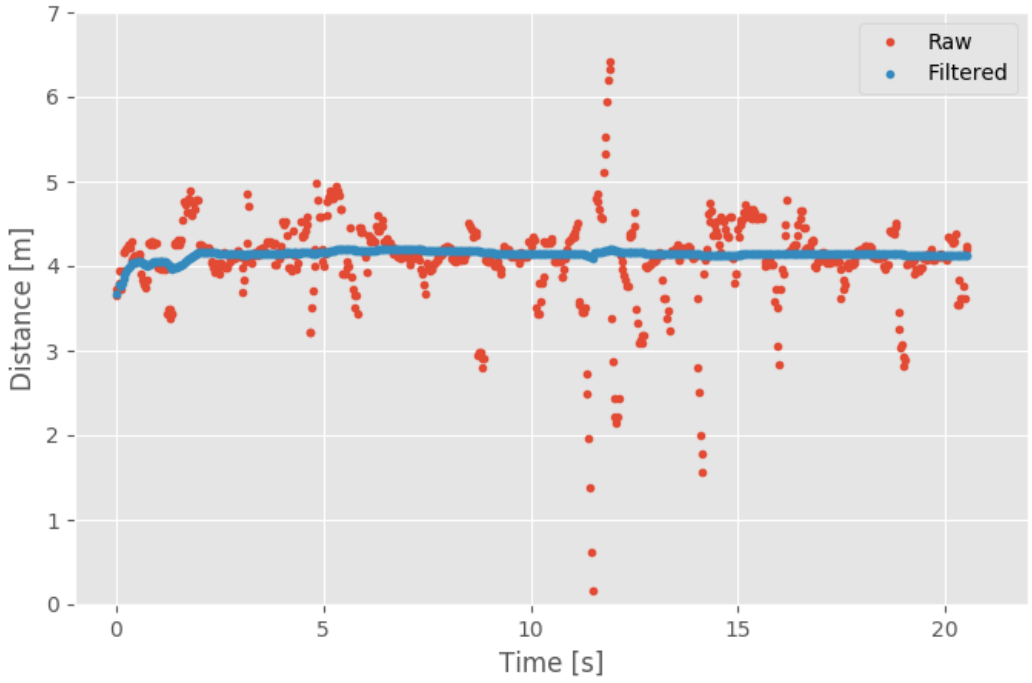

Figure A.2: Calculated Distance vs. Time for D = 4 m.

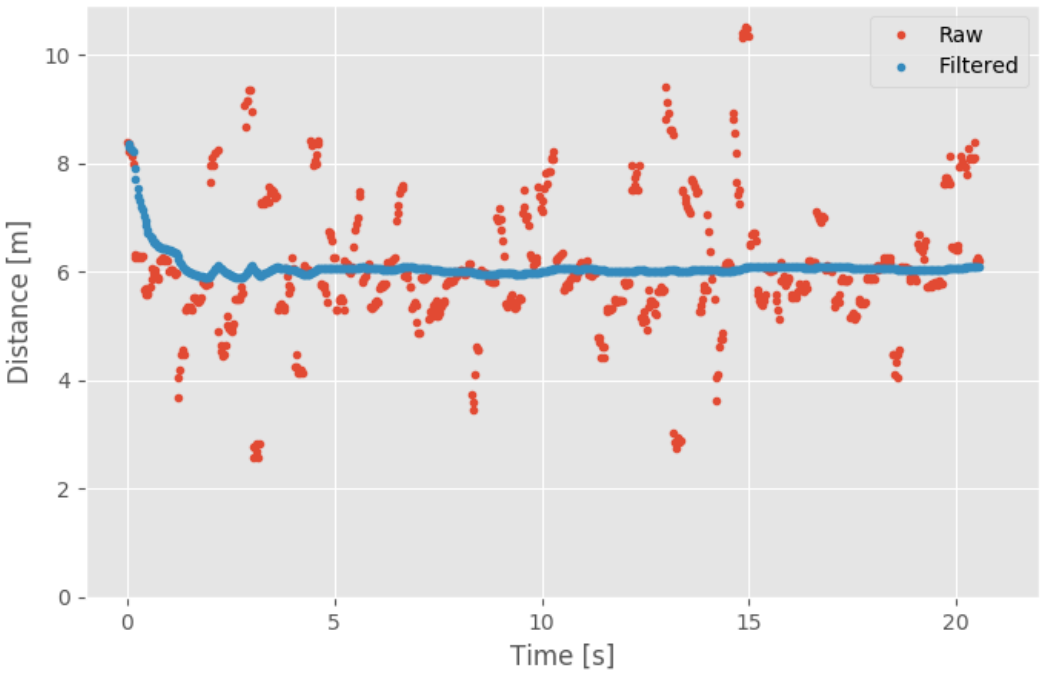

Figure A.3: Calculated Distance vs. Time for D = 6 m.

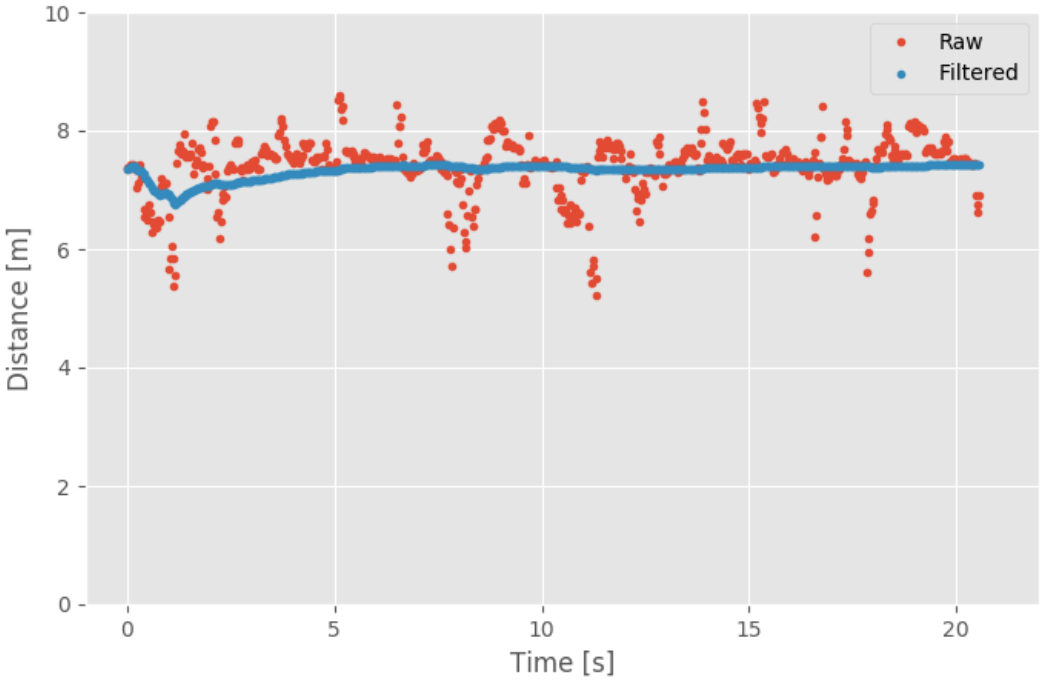

Figure A.4: Calculated Distance vs. Time for D = 8 m.

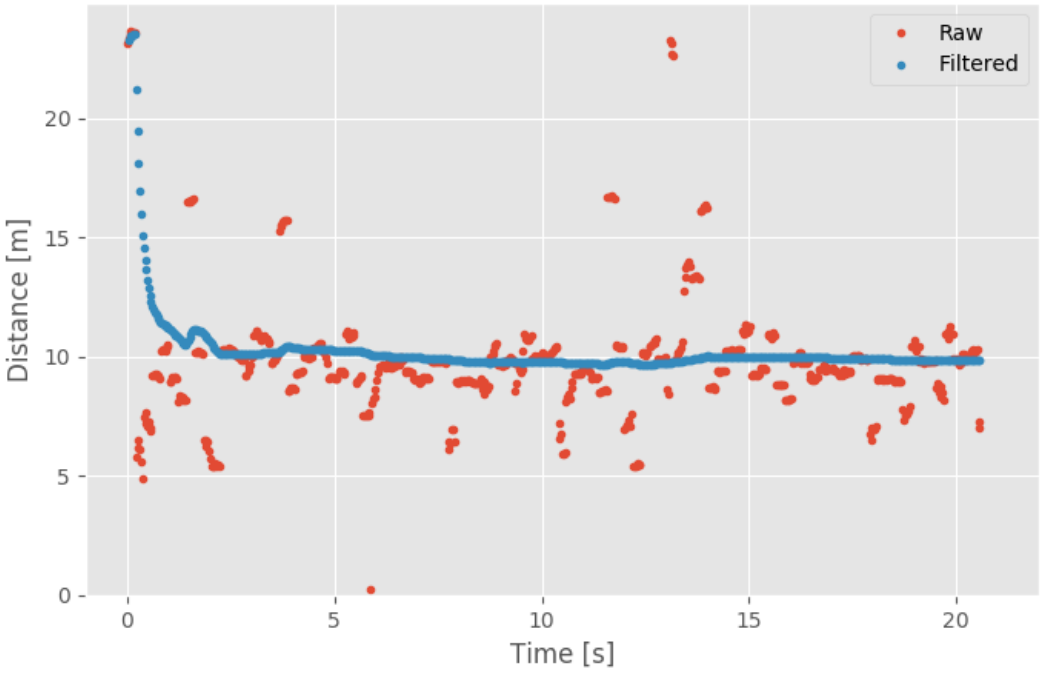

Figure A.5: Calculated Distance vs. Time for D = 10 m.

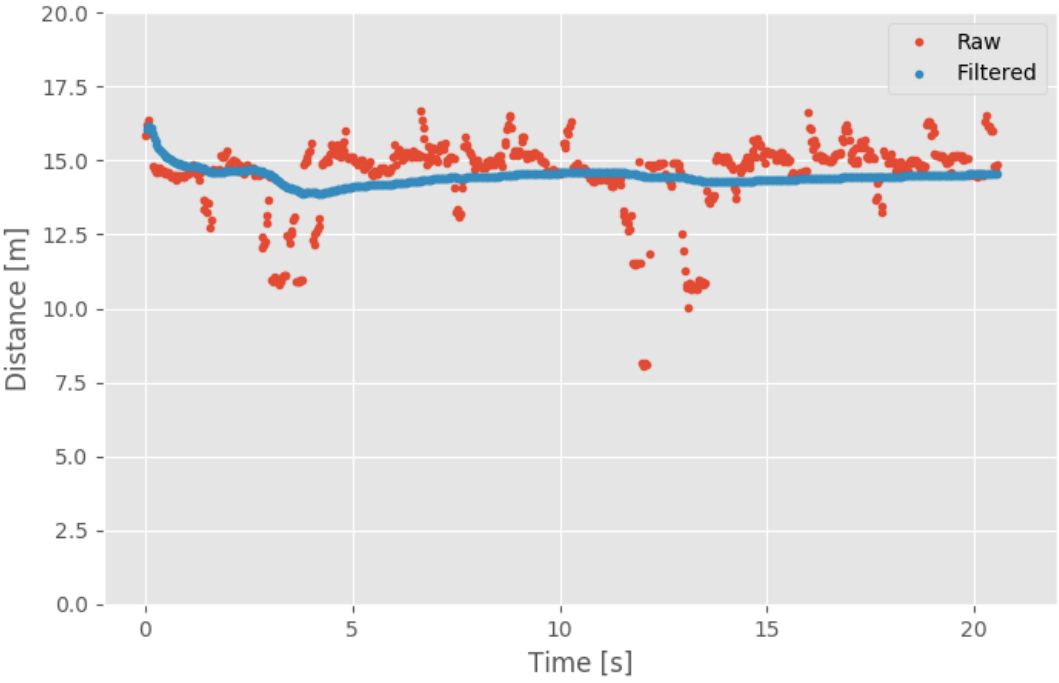

Figure A.6: Calculated Distance vs. Time for D = 15 m.

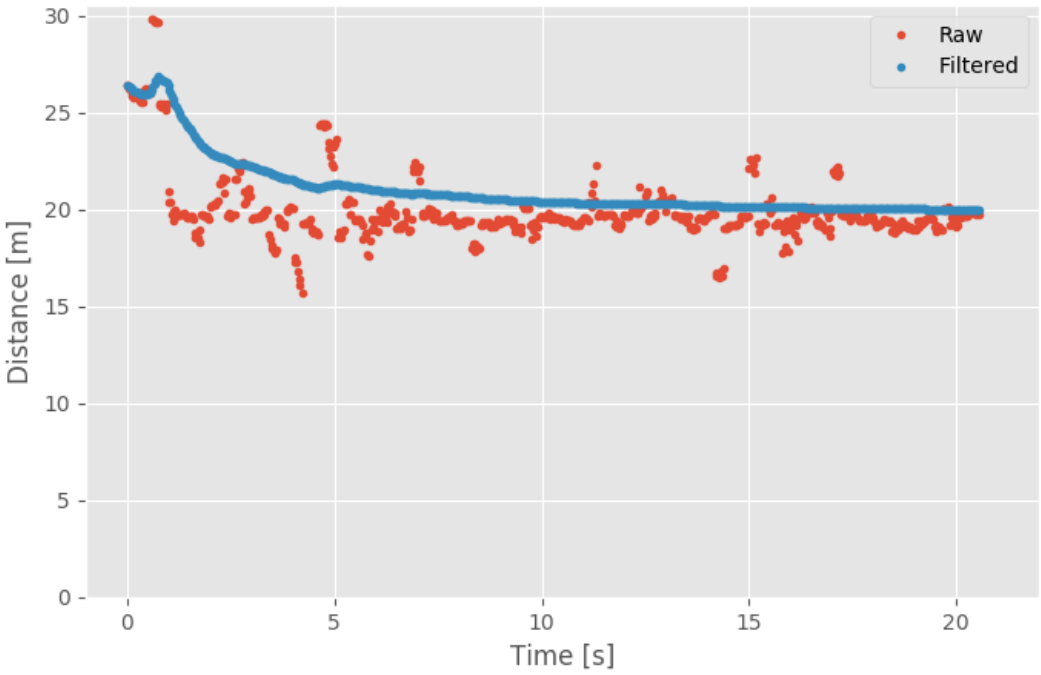

Figure A.7: Calculated Distance vs. Time for D = 20 m.

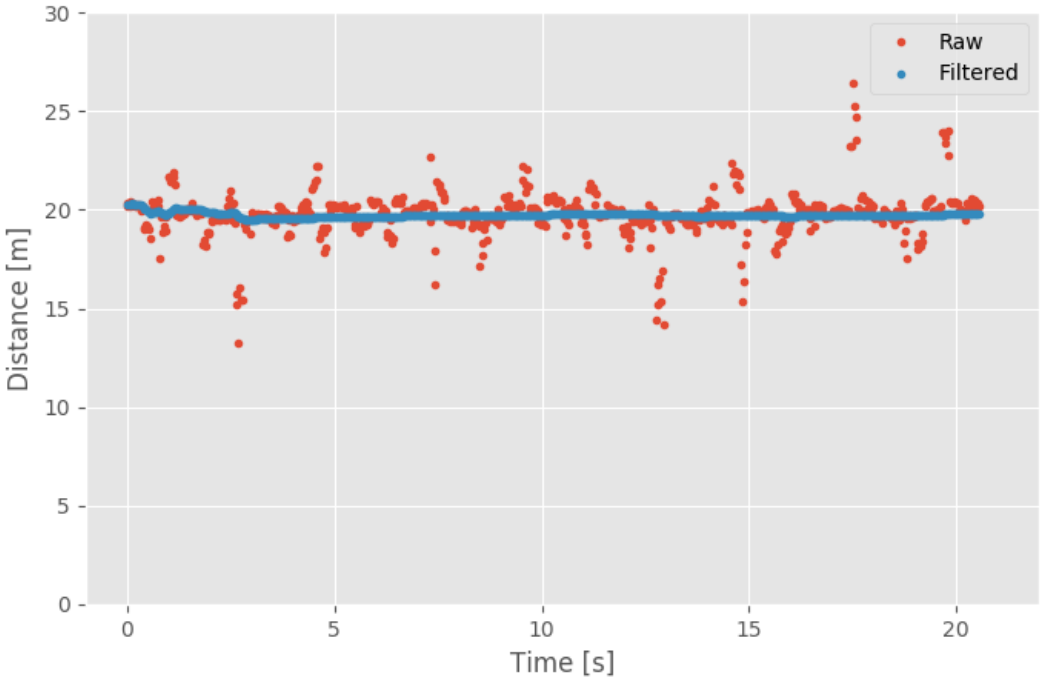

Figure A.8: Calculated Distance vs. Time for D = 20 m with an antenna angle of 22 degrees.

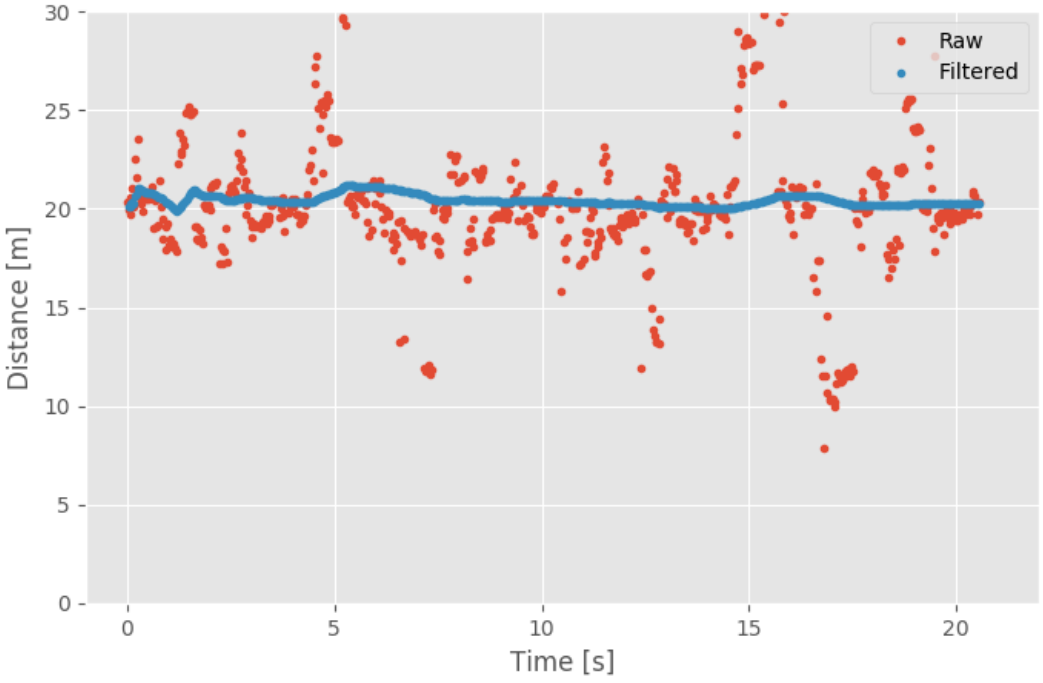

Figure A.9: Calculated Distance vs. Time for D = 20 m with an antenna angle of 45 degrees.

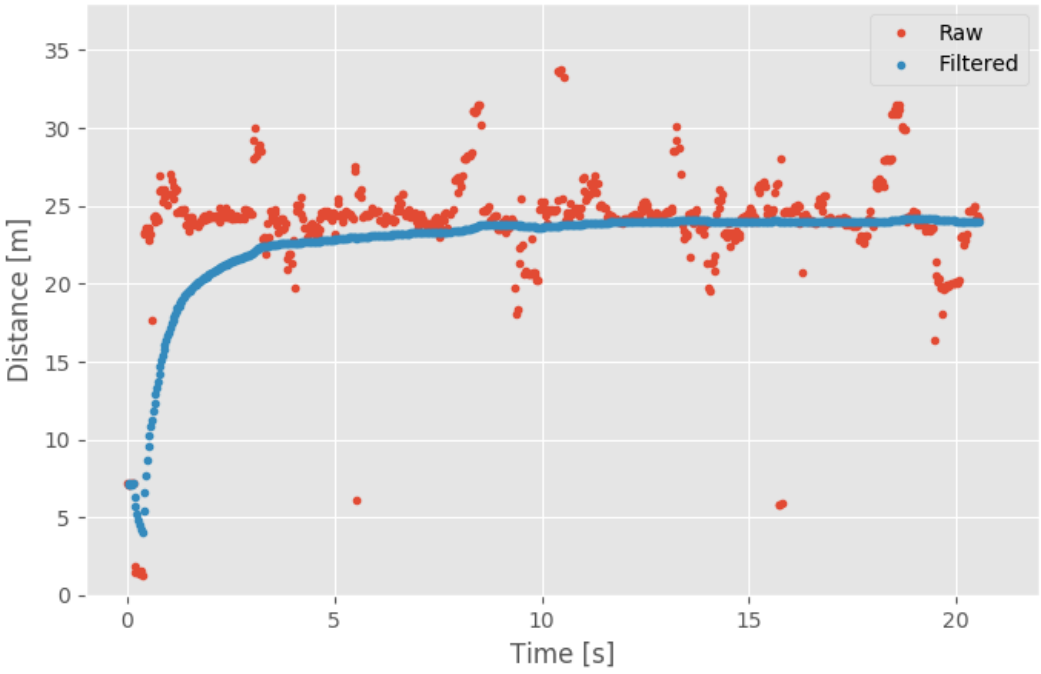

Figure A.10: Calculated Distance vs. Time for D = 25 m.

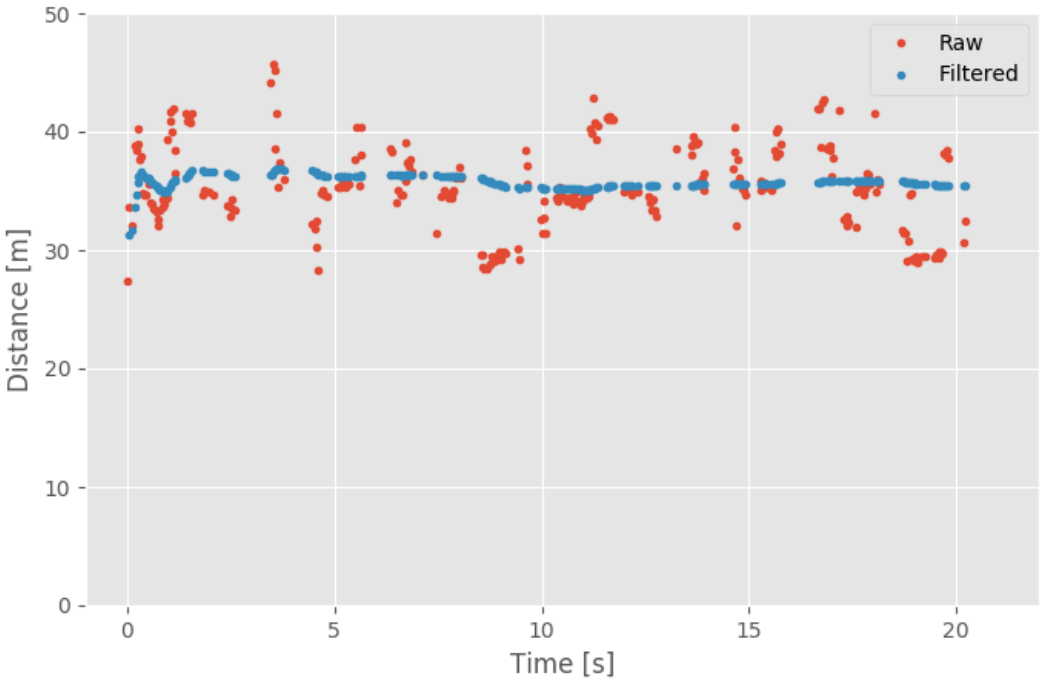

Figure A.11: Calculated Distance vs. Time for D = 35 m.

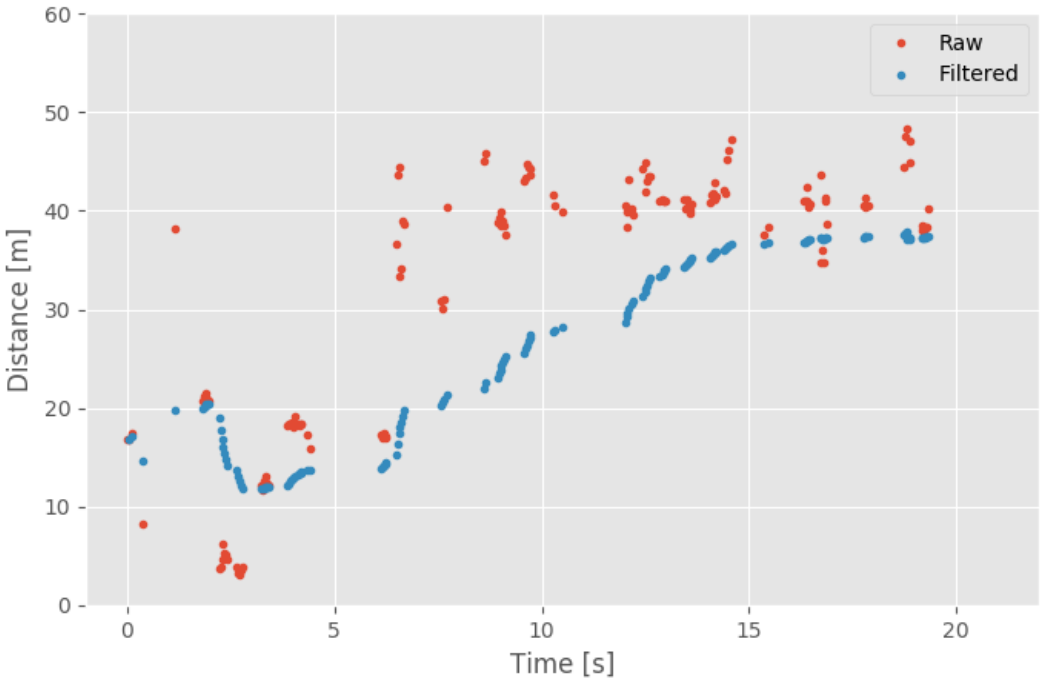

Figure A.12: Calculated Distance vs. Time for D = 40 m.

APPENDIX B

DYNAMIC TESTING FIGURES

Additional plots for the dynamic testing discussed in section 3.2.

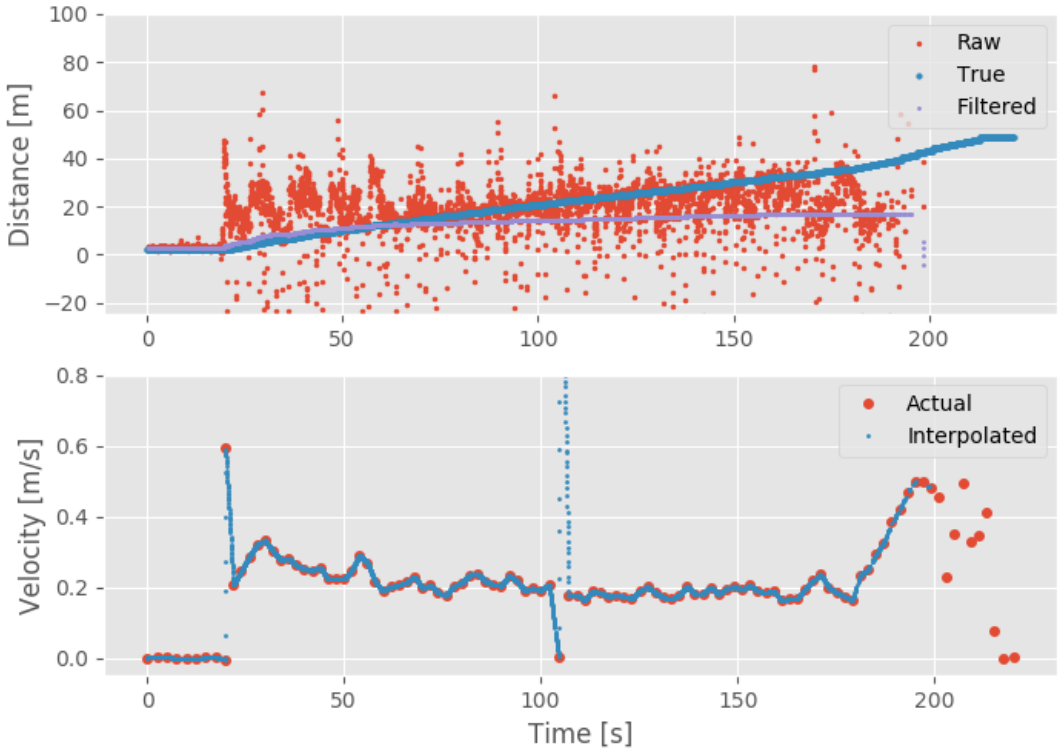

Figure B.1: Dynamic Test - Trial 2

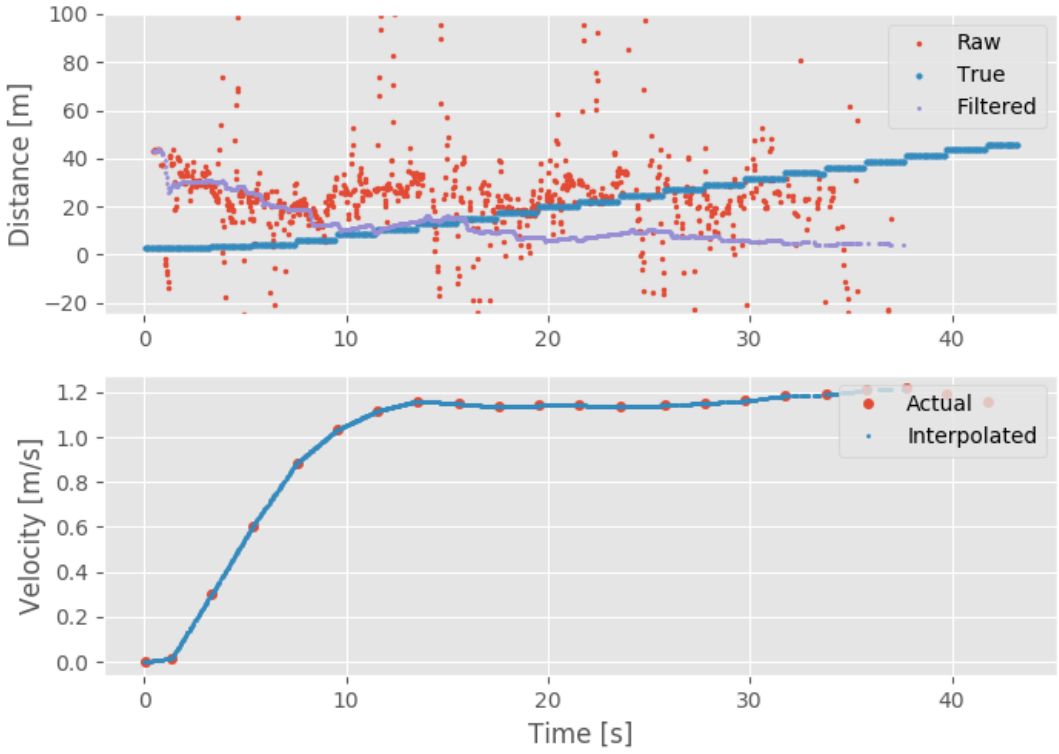

Figure B.2: Dynamic Test - Trial 4

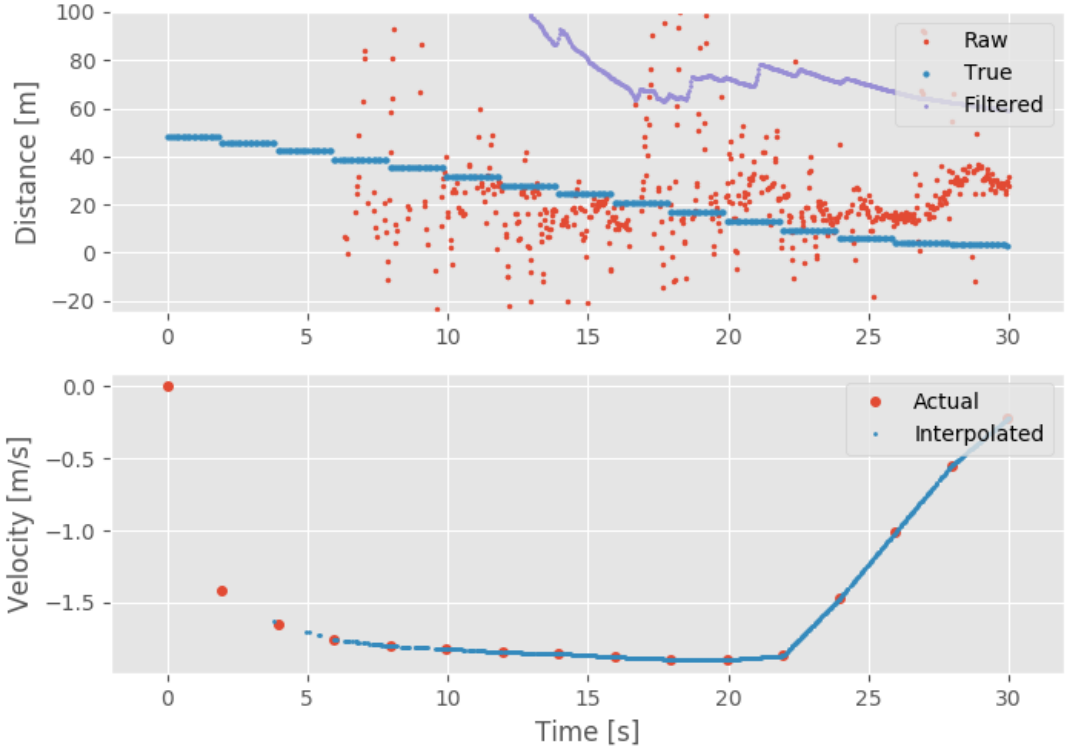

Figure B.3: Dynamic Test - Trial 5

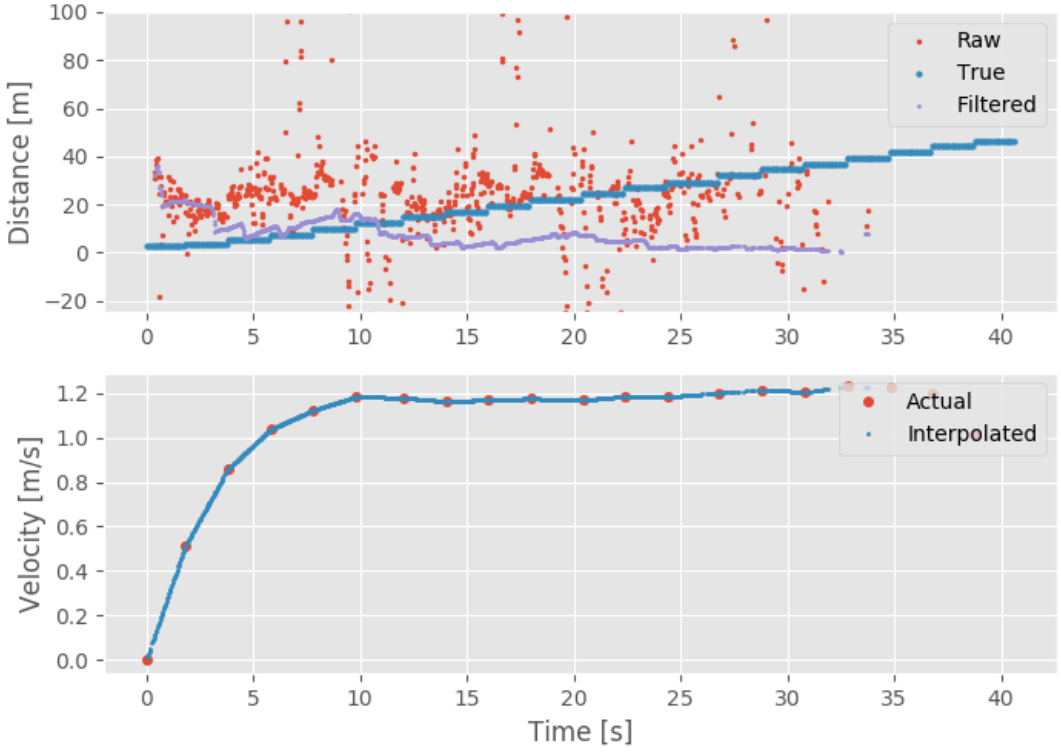

Figure B.4: Dynamic Test - Trial 6

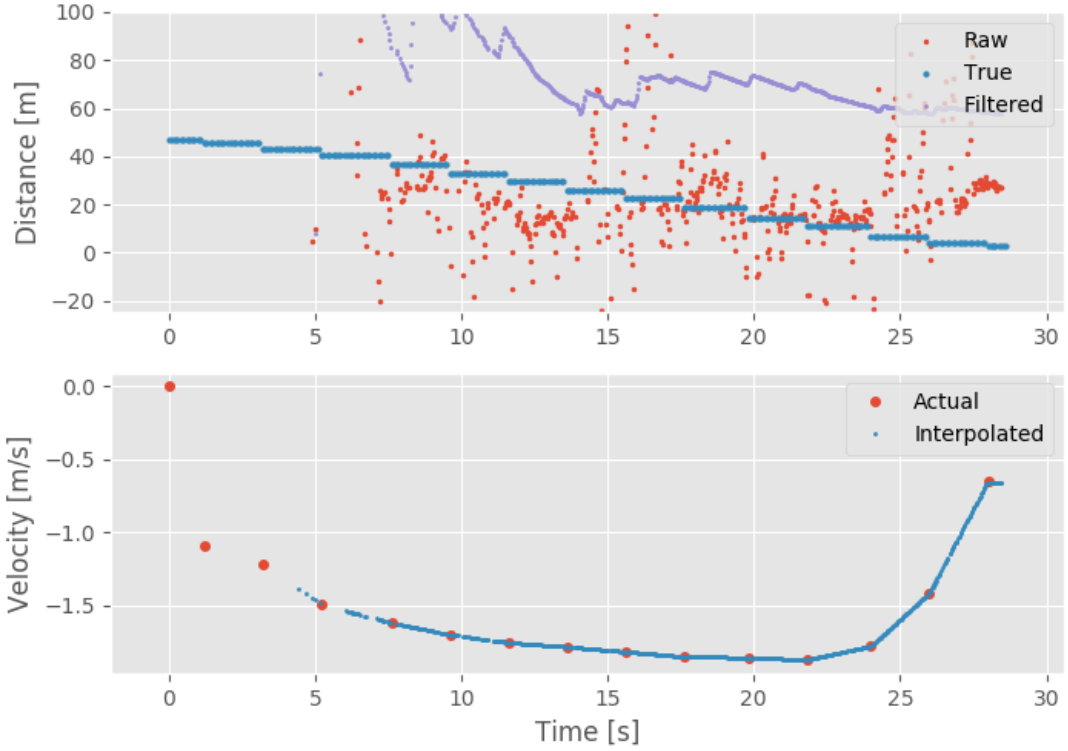

Figure B.5: Dynamic Test - Trial 7

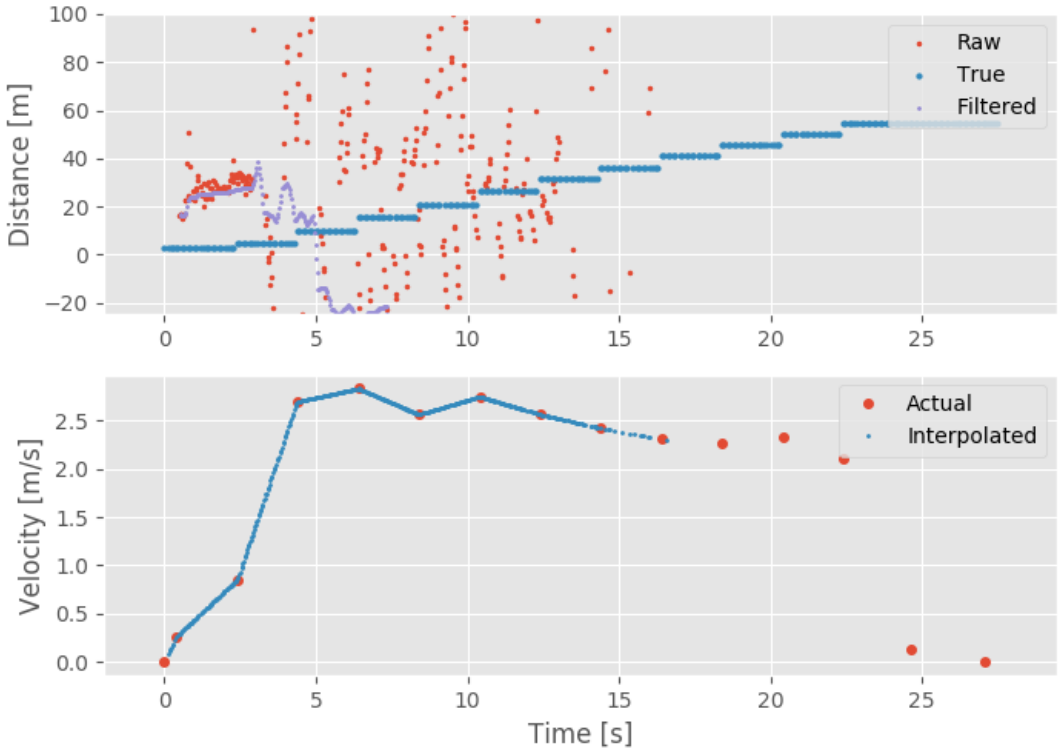

Figure B.6: Dynamic Test - Trial 8

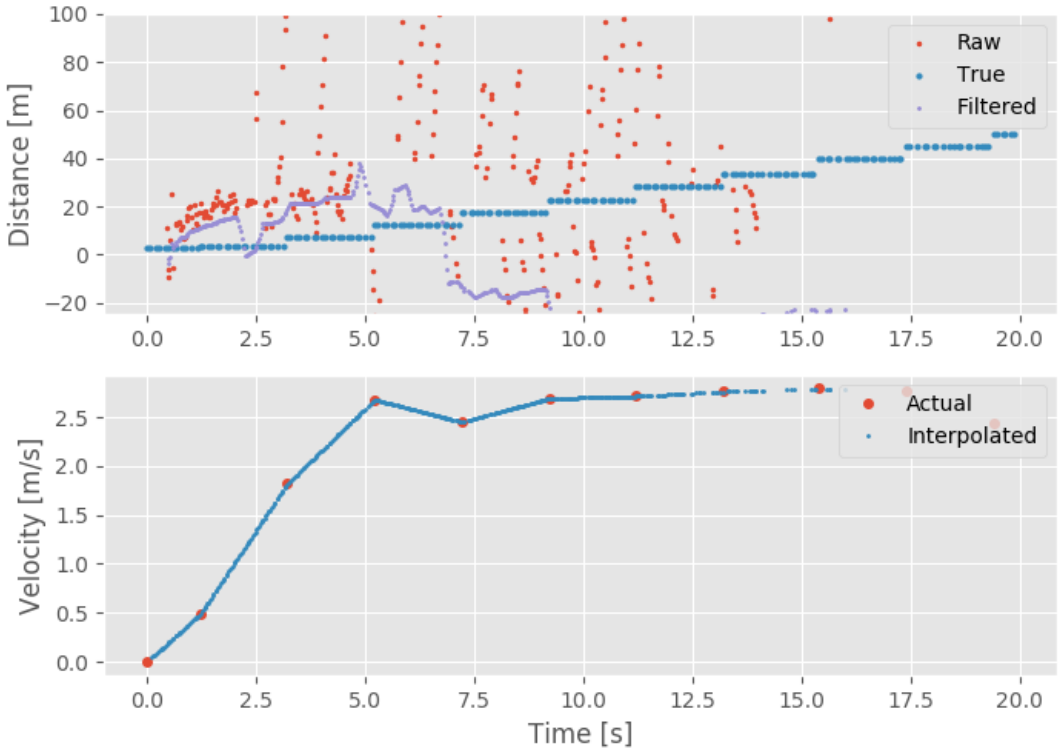

Figure B.7: Dynamic Test - Trial 9

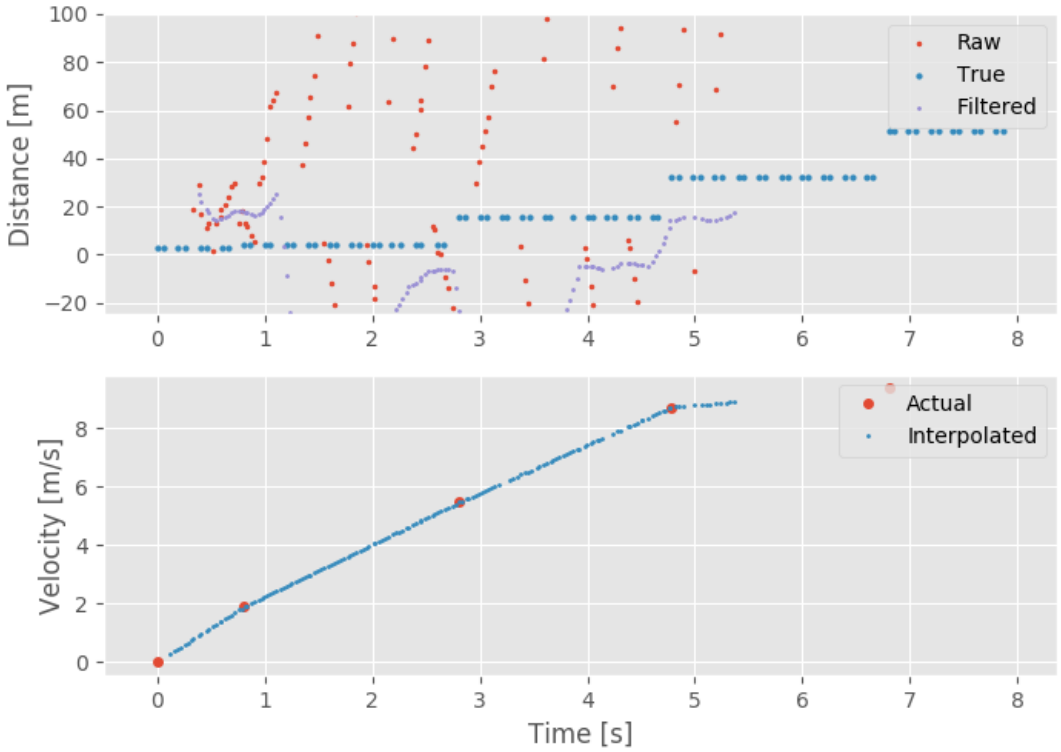

Figure B.8: Dynamic Test - Trial 10